energies

Article

Differential Reservoir-Forming Mechanisms of the Lower Paleozoic Wufeng-Longmaxi and Niutitang Marine Gas Shales in Northern Guizhou Province, SW China: Theories and Models

Wei Du [1,2], Wei Yang [3,4,*], Xingyu Li [3,4,*], Fulun Shi [1,2], Ruiqin Lin [1,2], Yisong Wang [1,2], Daquan Zhang [1,2], Yi Chen [1,2], Zhao Sun [1,2] and Fuping Zhao [1,2]

1 Key Laboratory of Unconventional Natural Gas Evaluation and Development in Complex Tectonic Areas, Ministry of Natural Resources, Guiyang 550001, China; duweiletian@126.com (W.D.); sfl860222@163.com (F.S.); krlinrq@163.com (R.L.); wangyisong199133@163.com (Y.W.); daquan0807@163.com (D.Z.); cy18800135772@163.com (Y.C.); sz15600363611@163.com (Z.S.); zhaofupinggui@163.com (F.Z.)
2 Guizhou Engineering Research Institute of Oil & Gas Exploration and Development, Department of Natural Resources of Guizhou Province, Guiyang 550001, China
3 State Key Laboratory of Petroleum Resources and Prospecting, China University of Petroleum, Beijing 102249, China
4 Unconventional Natural Gas Institute, China University of Petroleum, Beijing 102249, China
* Correspondence: yangw@pku.edu.cn (W.Y.); 2020216435@student.cup.edu.cn (X.L.); Tel./Fax: +86-10-89739051 (W.Y.)

Citation: Du, W.; Yang, W.; Li, X.; Shi, F.; Lin, R.; Wang, Y.; Zhang, D.; Chen, Y.; Sun, Z.; Zhao, F. Differential Reservoir-Forming Mechanisms of the Lower Paleozoic Wufeng-Longmaxi and Niutitang Marine Gas Shales in Northern Guizhou Province, SW China: Theories and Models. *Energies* **2022**, *15*, 5137. https://doi.org/10.3390/en15145137

Academic Editors: Manoj Khandelwal and Prabir Daripa

Received: 6 May 2022
Accepted: 7 July 2022
Published: 15 July 2022

Abstract: Fine dissection of microscopic pore structure variations between the Niutitang Formation and the Wufeng-Longmaxi Formation will help to improve the understanding of the underlying geological theory of shale gas in northern Guizhou Province. The stratigraphic, geochemical, physical, and tectonic properties of the two formations vary greatly, resulting in differential development of the microscopic pore structure among reservoirs and, as a result, major variances in gas concentration. To explore the mechanism of differential pore evolution, experimental techniques and instruments such as gas adsorption, liquid intrusion, SEM, XRD, and organic geochemical tests were utilized. The results indicate that the Wufeng-Longmaxi Formation is in a high-maturity stage, while the Niutitang Formation is in an over-mature stage. The latter has a higher TOC content. Both petrographic phases are siliceous shale petrographic phases, and the former has more developed dissolution pores with better pore volume, throat radius, and macropore pore diameters than the latter, as well as organic matter pores, intergranular pores, and microfracture structural parameters, whereas the specific surface area is the opposite. The differences in reservoir pore formation between the two formations were analyzed, and the results showed that the petrographic type, thermal evolution, and tectonic preservation conditions were the primary controlling elements of differential shale gas reservoir formation. A differential reservoir-forming model of the Wufeng-Longmaxi Formation and the Niutitang Formation was constructed, providing a geological and theoretical basis for shale gas geological exploration in northern Guizhou Province.

Keywords: organic matter pores; pore structure; characteristic parameters; pore development characteristics; main controlling factors; Wufeng-Longmaxi Formation; Niutitang Formation; differential reservoir-forming model

1. Introduction

Currently, shale gas is emerging as the fastest-growing maverick natural gas resource in the world and will likewise be China's fundamental source of natural gas production growth in the next five to ten years [1,2]. The Upper Yangzi region is a favorable area for shale gas development in China [3,4], especially in the Sichuan Basin and its periphery, which has favorable geological conditions and is the region where Chinese shale gas exploration has made a forward leap [5]. Seven key exploration development zones have been established, namely, Fuling, Changning, Weiyuan, Zhaotong, Qijiang, Weirong, and Taiyang. The prospecting and exploitation of shale gas in northern Guizhou Province are likewise abundant; however, they face challenges due to extremely complex tectonic features. Given this explanation, we investigated the physical properties of the reservoir, the evolution of pore structure, and its major controlling factors for the shales of the Wufeng-Longmaxi and Niutitang Formations in northern Guizhou Province.

The pore structure diversity of the Niutitang and Longmaxi Formations is the principal constraint to the exploitation of shale gas in northern Guizhou Province. The shale gas reservoirs of the Lower Cambrian Qiongzhusi Formation and the Lower Silurian Longmaxi Formation in the southern Sichuan Basin are dominated by extremely well-developed micropores, which provide a large pore volume and specific surface area, whereas the specific surface area and the pore volume of the mesopores and macropores of the shales of the Qiongzhusi Formation are more modest than those of the Longmaxi Formation [6,7]. Interestingly, the mesopores and macropores of the shales of the Longmaxi Formation are relatively evolved, while the micropores of the shales of the Niutitang Formation are more evolved. The pore size of the Longmaxi Formation shales is essentially at the nanoscale, and the pore types can be classified into organic matter pores, inorganic matter pores, and microfractures, with organic matter pores and intergranular pores of clay minerals being the most broadly distributed [8,9]. The pore structure of the Niutitang Formation is made up of ink-bottle-shaped pores, parallel slit-like pores, and a small number of fissure-like pores [6,10,11]. The pores are generally open, essentially cylindrical, and parallel slab-like and slit-like with four open sides [12–15]. The pore structure of the two formations in northern Guizhou Province has been subjected to more complicated tectonic movements than the interior of the Sichuan Basin, resulting in differences in pore structure, but there is still insufficient investigation on the distinctions in pore structure between the two shale formations in northern Guizhou Province, and further analysis is necessary.

Organic matter is one of the constraints impacting the pore structure of shale [16]. The pores developed within the organic matter greatly enhance the shale's specific surface area and volume, which become the main carrier for adsorbed gas [17]. Organic matter pores have good connectivity [16,18–21]. Compared with the shales of the Wufeng-Longmaxi Formation, the shape coefficients of the organic matter pores of the Niutitang Formation shales are lower and deviate to a greater extent from the surrounding pores. The pore long-axis direction of the Longmaxi Formation shales is more consistent with the organic matter extension direction [22]. The organic matter pore variability among shales is well studied in most parts of the Sichuan Basin; however, the organic matter pore structure and its variability in the two layers in northern Guizhou Province still need further exploration.

Shale pore structure distinctions are essentially affected by mineral composition, organic matter type, organic carbon content, thermal evolution degree, preservation conditions, and other factors. The degree of thermal evolution has the most pronounced effect [7,23–26]. As the degree of thermal evolution, organic carbon content, and clay mineral content rise, the number of microscopic pores, the specific surface area, and pore volume increase [16,27,28]. Shale petrography, the degree of thermal evolution, tectonics, and preservation conditions have significant influences on the pore structure; within a certain range, the specific surface area and pore volume of organic matter pores in mud shale increase with increasing thermal evolution, while the specific surface area and pore volume of micropores between clay minerals decrease with increasing thermal evolution [7,29]. The shales can be partitioned into assorted phases according to their mineral type and content, with clayey shales growing more clay mineral flake-like intragranular pores that are mostly filled with organic matter, mixed shales developing more organic matter pores and carbonate mineral dissolution macropores, and siliceous shales growing more organic matter pores. The mean values of the total porosity ratio, pore volume, and pore specific surface area for mixed shales are similar to those of siliceous shales. Organic-rich siliceous shales have a high proportion of micropores, a high contribution to the specific surface area, and the largest pore volume and specific surface area, which are conducive to shale gas enrichment [30]. Pore structure evolution is caused by the difference in movement intensity caused by later uplift. The intensity of tectonic transformation is the key controlling element of the preservation conditions of shale gas, and a broad and gentle tectonic style, continuous caprock, and tectonic background facilitate the accumulation of shale gas. The pore size, shape, and porosity reflect the preservation conditions to a certain extent; in ideal preservation conditions, shale pores have larger pore sizes and are mostly rounded or bubble-shaped, while in damaged preservation conditions, shale pores have relatively undeveloped pore sizes and a variety of shapes, which are mostly flattened or polygonal or have some flattened and deformation characteristics. The pore volume and specific surface area of well-preserved black shale are better than those of black shale where preservation conditions have been compromised [31,32]. The Wufeng-Longmaxi Formation and the Niutitang Formation have been affected by multiple phases of tectonic movement in northern Guizhou Province, resulting in various variations in petrography, thermal evolution, and tectonic preservation conditions compared to the interior of the Sichuan Basin. The mechanisms of their impact on the differences in pore structure between the Wufeng-Longmaxi and Niutitang Formations in northern Guizhou Province are obscure and require further examination.

We examined the multi-scale pore structures and pore types of the shales in the Wufeng-Longmaxi and Niutitang Formations in northern Guizhou Province and revealed the pore structure differences between the Wufeng-Longmaxi and Niutitang Formation. Then, we determined the comprehensive evaluation parameters of organic matter pores, intergranular pores, and microfracture development characteristics and analyzed the factors controlling the pore structure differences. Finally, we established a model for differential reservoir pore formation in the two target formations. The results provide a geological and theoretical basis for the commercial development of shale gas in northern Guizhou Province.

2. Geological Setting

The research area is situated in northern Guizhou Province and at the southeastern edge of the Sichuan Basin. It is delimited by the Zunyi–Nanchuan Fault to the east and the Guiyang–Zhenyuan Fault to the north, with the provincial boundary of the Guizhou Province administrative region to the north and east. The periodic crustal movement transformed Guizhou Province from an oceanic crust to a continental margin transitional crust, which finally evolved into a continental crust. The Xuefeng movement caused the continental crust to re-degrade to a continental margin transitional crust after tectonic activation, and it evolved into the continental crust at the end of the Caledonian movement. The Hercynian–Indo–Chinese movement stage was an active continental crust in a shallow platform environment. In the Yanshanian–Himalayan stage, the continental crust was activated in the terrestrial environment [33]. As shown in Figure 1 [34], The fracture system in northern Guizhou Province was formed by the mutual cutting, uniting, and interference of multiple trending fractures, with the fractures and folds striking mostly in the north-east and north-northeast directions and the individual folds being "S"-shaped or anti-"S"-shaped, indicating that the tectonic deformation in northern Guizhou Province is dominated by compression and strike-slip [35].

The exposed strata in the study area are mainly Nanhua, Sinian, Cambrian, Ordovician, Silurian, and Permian. The distribution of Silurian and Permian is limited. The Longmaxi Formation of the Lower Silurian System was affected by the ancient uplift in central Guizhou Province. The strata in the southern region are partially absent and eroded, and the Cambrian is widely distributed. The Lower Cambrian Niutitang Formation's buried depth is, for the most part, huge in the eastern Wuchuan syncline, around 2000–3000 m. The buried depth of the Xieba anticlinorium in the western part of the study area is around 700–2000 m. The stratigraphic thickness of the Niutitang Formation in the study area is 128–146 m, which shows a trend of being thick in the northwest and thin in the southeast. The burial depth of the Longmaxi Formation is relatively shallow compared to that of the Niutitang Formation, and the depth of burial is principally along the syncline from the two flanks to the core; the maximum burial depth occurs at the core of the composite synchronized line. The Lower Silurian Longmaxi Formation is in a shallow shelf sedimentary environment [36], and the Lower Cambrian Niutitang Formation is in a deep-shelf sedimentary environment [37].

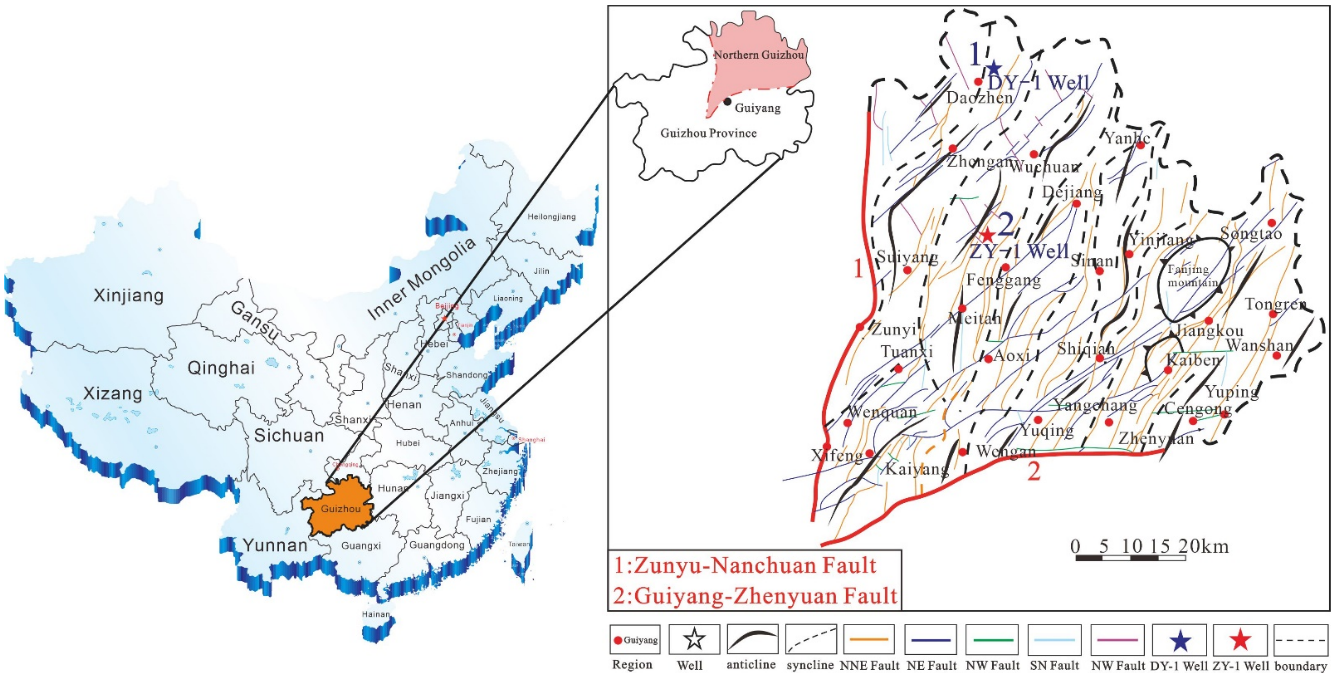

Figure 1. Tectonic outline map of northern Guizhou Province (modified after [34]).

3. Sampling, Methodology, and Data Processing Principles

The shale samples collected in well Daoye 1 (DY-1) and well Zhengye 1 (ZY-1) are from the Wufeng-Longmaxi Formation and Niutitang Formation, which are located in the Daozhen syncline and Xieba anticlinorium, respectively. The depths of the core samples in the Wufeng-Longmaxi Formation and Niutitang Formation ranged from 381.26 to 597.15 m and 970.675 to 1022.71 m, respectively. It is worth noting that the target samples that we selected were all located in the high-yield shale gas interval in northern Guizhou. Firstly, shale gas production in the high-yield shale interval is abundant, especially the higher free gas content. Secondly, based on the previous exploration practice in the northern Guizhou area, it is believed that the hydrocarbon generation intensity of the high-yield interval is higher and the storage conditions are better.

3.1. Organic Petrography and Mineralogy

The total organic carbon (TOC) and mineral composition of shale samples were determined and analyzed using a Vario EL III CHNOS analyzer (Langenselbold, Germany) and D8 DISCOVER X-ray diffractometer, respectively.

To determine the total organic carbon, first, the shale samples were cut into small pieces with the instrument and then crushed. The samples were ground into a 60-mesh powder (<250 mm), and then 100 mg of crushed samples was treated with concentrated hydrochloric acid for 2 h to remove carbonate minerals and then dried for analyzer tests.

The thermal maturity was measured through the vitrinite reflectance technique and expressed as Ro%. The sample was crushed into smaller 2–3 mm pieces. The sample was ground using abrasive powder. After sample preparation, a vitrinite random reflectance analysis was performed at a magnification of 500× using a Carl Zeiss Axio Imager microscope M2m for incident light equipped with an Illuminator micro LED lamp and a

50×/1.0 Epiplan-NEOFLUAR oil immersion objective; the analysis was carried out with a 1.518 refractive index at 23 °C and a 546 nm filter. Standard glass with a reflectance value of 1.250 Ro% was used to calibrate the instrument. Fifty-five points were measured on each sample to reach sufficient accuracy of vitrinite reflectance.

To analyze the mineralogical composition and different clay minerals, the shale samples were milled into less than 200-mesh powders and tested by X-ray diffraction. The percentage of minerals in shale samples was estimated semi-quantitatively from the Lorentz polarization correction main peak area. After extensive research, the accuracy of XRD testing to determine the mineral composition in tight reservoirs was determined to reach more than 90%.

3.2. FIB-SEM and Image-Pro Plus

At present, in order to observe nanoscale pores, it is necessary to use argon ions to polish rock samples to achieve nanoscale surface flatness and to clearly identify the relationship between pore characteristics and mineral contact. Before scanning electron microscope observation, the shale surfaces were first mechanically polished using the Leica EM TXP target surfacing system until the surface roughness parameters of the sample (such as Ra and Rz) showed good polishing quality, and they were then milled by a Leica EM RES102 ion beam milling system with an accelerating voltage of 3 kV and a crushing time of 6–10 h. Samples were mounted onto SEM stubs using carbon paste and coated with carbon to provide a conductive surface layer. Each sample was inserted into a Zeiss Merlin field-emission scanning electron microscope (FE-SEM) for imaging with accelerating voltages of 1–2 kV and working distances of about 3.5–5.5 mm. In addition, dual Bruker Quantax energy-dispersive X-ray spectroscopy (EDS) detectors were installed in the Merlin FE-SEM for chemical analysis.

The organic matter pores of organic-rich shale under the scanning electron microscope were extracted by Image-Pro Plus (IPP) software, and six characteristic parameters of organic matter pore structure, namely, plane porosity, pore diameter, roundness, convex degree, elongation, and fractal dimension of the organic pores, were calculated. Through the IPP image processing software, quantitative pore data extraction was divided into the following three steps: ① image reference scale settings; ② pore identification in SEM images of shale; and ③ quantitative pore data extraction [38]. As shown in Figure 2, firstly, the image recognition scale was set according to the image scale of the shale sample; then, the organic matter pores of shale were identified by adjusting the image threshold, which was mainly determined to reflect the pore morphology of shale and highlight the organic matter pores of shale; then, the quantitative data of the shale image were extracted by particle analysis.

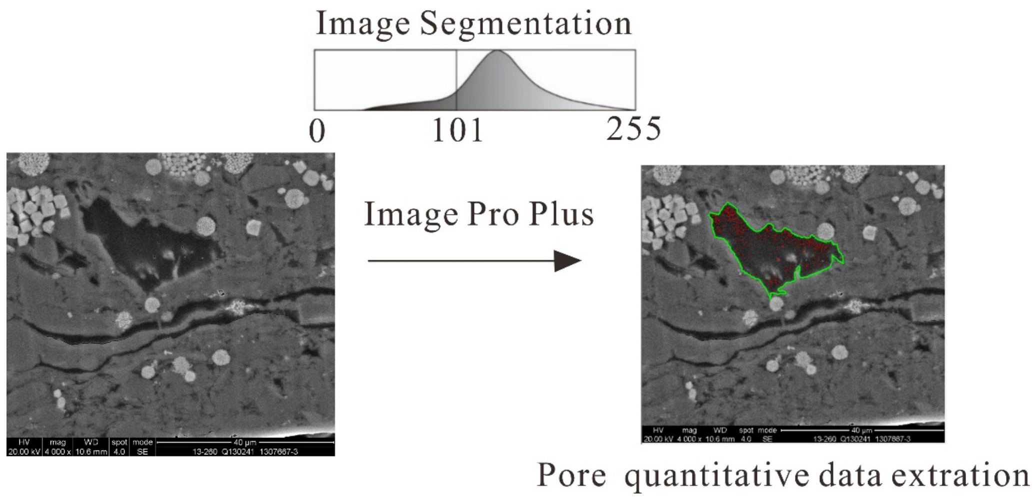

Figure 2. Pore extraction software flow.

3.3. High-Pressure Mercury Injection and Low-Pressure N_2 Adsorption Measurement

The high-pressure mercury injection apparatus uses the AutoPore IV9500 automatic mercury injection apparatus; the maximum working pressure is 413MPa, the aperture measurement ranges from 0.003~1000 μm, and the mercury injection volume measurement accuracy is 0.1 μL. Before the test, the shale sample was processed into core column fragments with a diameter of 3~10 mm and dried at 110 °C for 24 h to remove the free water and adsorbed water in the sample, and then the sample was vacuumized.

The basic principle of mercury intrusion to characterize rock pore structure and throats is that the mercury in the non-wetting phase must overcome the capillary force in the pore throats to enter the pore throats. The higher the displacement pressure, the greater the amount of mercury injected. That is, the higher the pressure, the smaller the corresponding pore throat radius.

The injection pressure of liquid mercury, as well as the pore size distribution, can be calculated by the following equation:

$$D = 2r = \frac{4\sigma\cos\theta}{p} \tag{1}$$

where D represents the pore size; θ is the wetting angle between mercury and the shale surface; σ is the surface tension of mercury; and P is the injection pressure of mercury [39].

Mercury saturation can be calculated by the following equation:

$$\Delta S_{Hg} = \frac{[(B_{i+1} - B_i) - (K_{bi+1} - K_{bi})] \times \alpha_V}{V_p} \times 100\% \tag{2}$$

where ΔS_{Hg} represents the mercury saturation increment; α_V is the change in volume represented by the unit measurement value of the mercury injection apparatus; B_i and B_{i+1} are the measured values reflecting the volumes at pressures of P_i and P_{i+1}; and K_{bi} and K_{bi+1} are the measured values reflecting the blank test volumes at pressures of P_i and P_{i+1}.

In the N_2 adsorption experiment, the Quantachrome Autosorb IQ instrument was used to analyze shale particle samples with a size of 40~60 mesh, and high-purity nitrogen was used as the adsorbent at low temperature (−196 °C). When nitrogen molecules with a molecular dynamic diameter of 0.364 nm enter the pore of the sample to be tested, they will be adsorbed on the pore surface, and micropore filling and capillary condensation will occur. Finally, measurements of the adsorption capacity of N2 under different conditions, which were created by changing the pressure value and the specific surface area, pore size distribution, and pore volume of shale samples, were acquired by the BET and BJH methods.

The adsorption amount of nitrogen molecules on the shale surface depends on the relative pressure of nitrogen. When $P/P_0 > 0.4$, capillary condensation will occur, and the influence of the shale pore size on the adsorption capacity cannot be ignored. The BJH equation is used to calculate the pore size of shale. The BJH equation is as follows:

$$r = -2 \times 10^9 \gamma V_m / \left[RT \ln\left(\frac{P}{P_0}\right)\right] + 0.354\left[-5/\ln\left(\frac{p}{p_0}\right)\right]^{\frac{1}{3}} \tag{3}$$

In the formula, "r" is the pore radius, nm; "γ" is liquid nitrogen surface tension, N/m; "V_m" is the molar volume of liquid nitrogen, m^3/mol; "R" is molar heat capacity, J/(K·mol); "T" is the experimental temperature, K; "P" is the partial pressure of nitrogen, Pa; and "P_0" is the saturated vapor pressure of nitrogen at liquid nitrogen temperature, Pa.

The BET equation is used to calculate the pore specific surface area of shale. The BET equation is as follows:

$$\frac{x}{V_{Ut}} = \frac{1}{V_m C} + \frac{(C-1)x}{V_m C} \tag{4}$$

In the formula, "x" is relative nitrogen pressure ($0.05 < x < 0.3$); V_m is the volume of nitrogen required by the multi-point method to form a single molecular layer on the surface of the sample to be tested per gram, mL/g; V_{ut} is the volume of adsorbed gas per gram of the sample to be tested (standard state), mL/g; and "C" is the constant of the BET equation.

3.4. Desorption Process

The desorption gas measurement was mainly completed at the drilling coring site. During the drilling process, the times at which the drilling started, the drill was lifted, the core arrived at the wellhead, and the tank loading was completed were accurately recorded. When the core was taken out of the wellhead, it was quickly loaded into the desorption tank, and the gap in the desorption tank was filled with fine-grained quartz sand before sealing. Then, it was put into a thermostatic device simulating the formation temperature to allow the core to naturally desorb in the desorption tank, and the desorption gas volume at different times was recorded until the end of desorption.

In the natural desorption method, desorption was measured for the first time within 5 min after the completion of canning, 1H every 10, 15, 30, and 60 min thereafter, and then twice every 120 min. After a cumulative total of 8 h, the appropriate desorption time interval could be determined according to the pressure gauge of the desorption tank; the longest was 24 h, and the desorption amount per balance was less than or equal to 10 cm^3 for 7 consecutive days, or the average desorption amount per gram of sample within a week was less than 0.05 cm^3/d, and the natural desorption ended.

4. Results

4.1. Organic Geochemical Characteristics

The TOC of the Wufeng-Longmaxi Formation and Niutitang Formation ranges from 0.23 to 4.11% and 4.65 to 19.29%. The vitrinite reflectance of the Wufeng-Longmaxi and Niutitang Formations located in the northern Guizhou Province ranges from 0.90 to 3.20% and 2.04 to 3.40%, with averages of 1.86% and 2.61%, respectively, indicating that the Wufeng-Longmaxi Formation and Niutitang Formation have reached high maturity and early over-maturity to late over-maturity, respectively (Table 1).

Table 1. Ro and TOC of the Wufeng-Longmaxi and Niutitang Formations in northern Guizhou Province.

Well	Formation	Sample ID	Depth/m	Ro/wt%	TOC/wt%
DY-1	Wufeng-Longmaxi	DY1-S11	381.26	0.90	0.23
		DY1-S41	521.11	1.56	0.54
		DY1-S61	564.3	1.68	0.86
		DY1-S66	570.5	1.66	1.50
		DY1-S71	573.5	1.65	3.17
		DY1-18	576.56	3.20	3.19
		DY1-S77	577.7	1.86	2.60
		DY1-S82	580.7	1.77	2.76
		DY1-S86	583.1	1.95	3.78
		DY1-S91	586.1	2.04	3.44
		DY1-S95	588.8	2.18	4.11
		DY1-S106	597.15	1.83	3.92
ZY-1	Niutitang	ZY1-S37	970.675	2.50	6.55
		ZY1-S43	978.02	2.52	6.20
		ZY1-S53	984.905	3.25	6.41
		ZY1-S73	999.25	2.51	4.65
		Q130114	1006.16	2.19	5.36
		Q130116	1010.05	2.04	7.70
		Q130117	1010.71	2.58	9.55
		Q130118	1011.51	2.45	8.09
		Q130119	1013.91	2.82	7.95
		Q130120	1018.35	2.37	8.62
		Q130123	1022.01	2.64	19.29
		Q130124	1022.71	3.40	12.22

The sapropel values of the Wufeng-Longmaxi and Niutitang Formations range from 6~16% and 96~99%, with averages of 10.5% and 98%. The vitrinite values of the Wufeng-Longmaxi and Niutitang Formations range from 1~5% and 0~4%, with averages of 2.7% and 1.5%. The organic matter of the Wufeng-Longmaxi shale does not contain inertinite, and the inertinite values of the Niutitang Formation range from 1~2%, with an average of 1.67%. To evaluate the quality of organic matter types, the type indexes of the Wufeng-Longmaxi and Niutitang Formations were calculated and found to range from 47~57 and 93~98.25%, with averages of 52 and 96.4, which indicate that the organic matter types of the Wufeng-Longmaxi and Niutitang shales are type II_1 and type I, respectively (Table 2).

Table 2. Kerogen microscopy in the Wufeng-Longmaxi and Niutitang Formations in northern Guizhou Province.

Well	Sample ID	Formation	Depth/m	Sapropel Group/wt%	Vitrinite/wt%	Inert Mass Group/wt%	Type	
							Type Index	Type
DY-1	DQ1 1-1	Wufeng-Longmaxi	/	12	3	/	52	II_1
	DQ1 2-1		/	10	2	/	53	II_1
	DQ1 3-1		/	16	1	/	57	II_1
	DQ1 4-1		/	9	2	/	52	II_1
	DQ1 5-1		/	6	5	/	47	II_1
	DQ1 6-1		/	10	3	/	51	II_1
ZY-1	ZY1 1-1	Niutitang	/	98	2	/	96.5	I
	ZY1 2-1		/	99	1	/	98.25	I
	ZY1 3-1		/	98	0	2	96	I
	ZY1 4-1		/	97	3	/	94.75	I
	ZY1 5-1		/	99	1	/	98.25	I
	ZY1 6-1		/	97	3	/	94.75	I
	ZY1 7-1		/	96	4	/	93	I
	ZY1 8-1		/	99	1	/	98.25	I
	ZY1 9-1		/	99	0	1	98	I
	ZY1 10-1		/	97	1	2	94.25	I
	ZY1 11-1		/	99	1	/	98.25	I
	ZY1 12-1		/	98	1	1	96.25	I

4.2. Mineralogy and Lithofacies

The mineral compositions of the Wufeng-Longmaxi and Niutitang shales were tested (Table 3). As shown in Table 3 and Figure 3, the silica minerals include potassium feldspar, plagioclase, and quartz; the carbonate minerals include anhydrite, dolomite, and calcite; and the clay minerals include kaolinite, chlorite, il/montmorillonite mixed layer, and illite. The mineral composition of the Wufeng-Longmaxi Formation is mainly quartz and clay minerals, and the main minerals of the Niutitang Formation are quartz and feldspar. Specifically, the contents of quartz in the shales of Wufeng-Longmaxi and Niutitang Formations are in the ranges of 32~76% and 31~61%, with averages of 44.5% and 42.5% (Figure 3a). The contents of feldspar are in the ranges of 8~27% and 21~44%, with averages of 16.7% and 29.6% (Figure 3a). The contents of carbonate are in the ranges of 4~20% and 2~27%, with averages of 16.7% and 9.5% (Figure 3b). The contents of pyrite are in the ranges of 0~8% and 0~9%, with averages of 2.4% and 5.1% (Table 3). The contents of clay are in the ranges of 10~35% and 0~28%, with averages of 24.5% and 13.3% (Figure 3c).

Based on organic geochemical features and mineral compositions, shales of the Wufeng-Longmaxi Formation and Niutitang Formation can be divided into six different facies (Table 4), namely, siliceous shale facies, clayey shale facies, calcareous shale facies, mixed clayey–siliceous shale facies, mixed clayey–calcareous shale facies, and mixed calcareous–siliceous shale facies. This method can effectively reflect the relationship between different mineral types and specific gravity in the shale formation. It can represent mineral types and proportion relationships between different minerals, which can directly reflect the sedimentary water conditions from the side, which provides useful guidance for the stratigraphic analysis of the Wufeng-Longmaxi and Niutitang Formations [40,41].

Table 3. Mineral compositions and contents of the Wufeng-Longmaxi and Niutitang Formations in northern Guizhou Province.

Well	Sample ID	Formation	Depth/m	Quartz/wt%	Potassium Feldspar/wt%	Plagioclase/wt%	Calcite/wt%	Dolomite/wt%	Pyrite/wt%	Anhydrite/wt%	Thenardite/wt%	Clay Minerals/wt%
DY-1	DY1-S11	Wufeng-Longmaxi	381.26	40	0	14	5	0	0	0	6	35
	DY1-S21		469.365	35	0	13	14	6	0	0	0	32
	DY1-S31		504.45	32	3	12	16	4	0	0	0	33
	DY1-S41		521.11	34	5	11	8	4	3	4	0	31
	DY1-S47		534.89	36	4	19	11	8	3	0	0	19
	DY1-S53		546.6	40	0	15	8	5	0	0	0	32
	DY1-S57		555.64	39	5	14	7	5	0	0	0	30
	DY1-10		560.585	42	4	13	6	4	0	0	0	31
	DY1-S61		564.3	44	4	14	8	6	0	0	0	24
	DY1-S66		570.5	45	6	21	5	3	0	0	0	20
	DY1-S71		573.5	48	3	9	6	7	5	0	0	22
	DY1-18		576.625	44	3	11	7	5	5	0	0	25
	DY1-S77		577.7	50	4	13	7	7	4	0	0	15
	DY1-S82		580.7	42	3	10	7	4	7	0	0	27
	DY1-S86		583.1	48	4	12	3	3	8	0	0	22
	DY1-S91		586.1	63	4	10	2	2	4	0	0	15
	DY1-24		588.365	39	5	14	2	14	5	0	0	21
	DY1-S95		588.8	42	7	18	3	7	6	0	0	17
	DY1-S99-1		591.9	76	2	6	4	2	0	0	0	10
	DY1-S103		594.775	55	4	10	2	6	0	0	0	23
	DY1-S106		597.15	41	5	16	3	5	0	0	0	30
ZY-1	ZY1-1	Niutitang	946.38	47	0	23	2	0	0	0	0	28
	ZY1-5		960.43	31	0	21	2	25	4	0	0	17
	ZY1-11		969.50	36	0	31	6	5	9	0	0	13
	ZY1-13		974.30	42	11	18	5	4	5	4	0	11
	ZY1-16		978.20	38	11	24	5	0	5	4	0	13
	ZY1-17		979.30	42	10	17	5	0	6	4	0	16
	ZY1-19		981.50	48	9	17	3	3	5	0	0	15
	ZY1-23		984.50	61	9	20	3	2	5	0	0	0
	ZY1-27		990.43	44	7	23	8	2	7	0	0	9
	ZY1-S69		996.15	33	13	31	4	3	6	0	0	10
	ZY1-34		1000.20	45	10	21	3	0	4	3	0	14

Table 4. Marine shale lithofacies division scheme.

Lithofacies Types	Mass Fraction of Mineral Components/wt%		
	Siliceous	Calcium	Clay
Siliceous shale facies	50~75	<30	10~50
Clayey shale facies	25~50	<30	50~75
Calcareous shale facies	<30	50~75	25~50
Mixed clayey–siliceous shale facies	30~50	<33	30~50
Mixed clayey–calcareous shale facies	<33	30~50	30~50
Mixed calcareous–siliceous shale facies	30~50	30~50	<33

According to the mineral composition data of two wells (DY-1 and ZY-1) in the north of Guizhou Province, the lithofacies division of the Wufeng-Longmaxi and Niutitang Formations in northern Guizhou Province was established (Figure 4).

Most of the shale samples from the Wufeng-Longmaxi Formation belong to the siliceous shale facies, with a small number belonging to mixed clayey–siliceous shale facies (Figure 4), and the content of carbonate minerals is higher than that of the Niutitang Formation. The TOC of the Wufeng-Longmaxi Formation is abundant (with an average of 2.5%). As for the Niutitang Formation, it all belongs to the siliceous shale facies; its siliceous content (52~90%) is higher than that of the Wufeng-Longmaxi Formation (Figure 4), and the contents of calcium and clay minerals are generally lower than those of the Wufeng-Longmaxi Formation (Figure 3d).

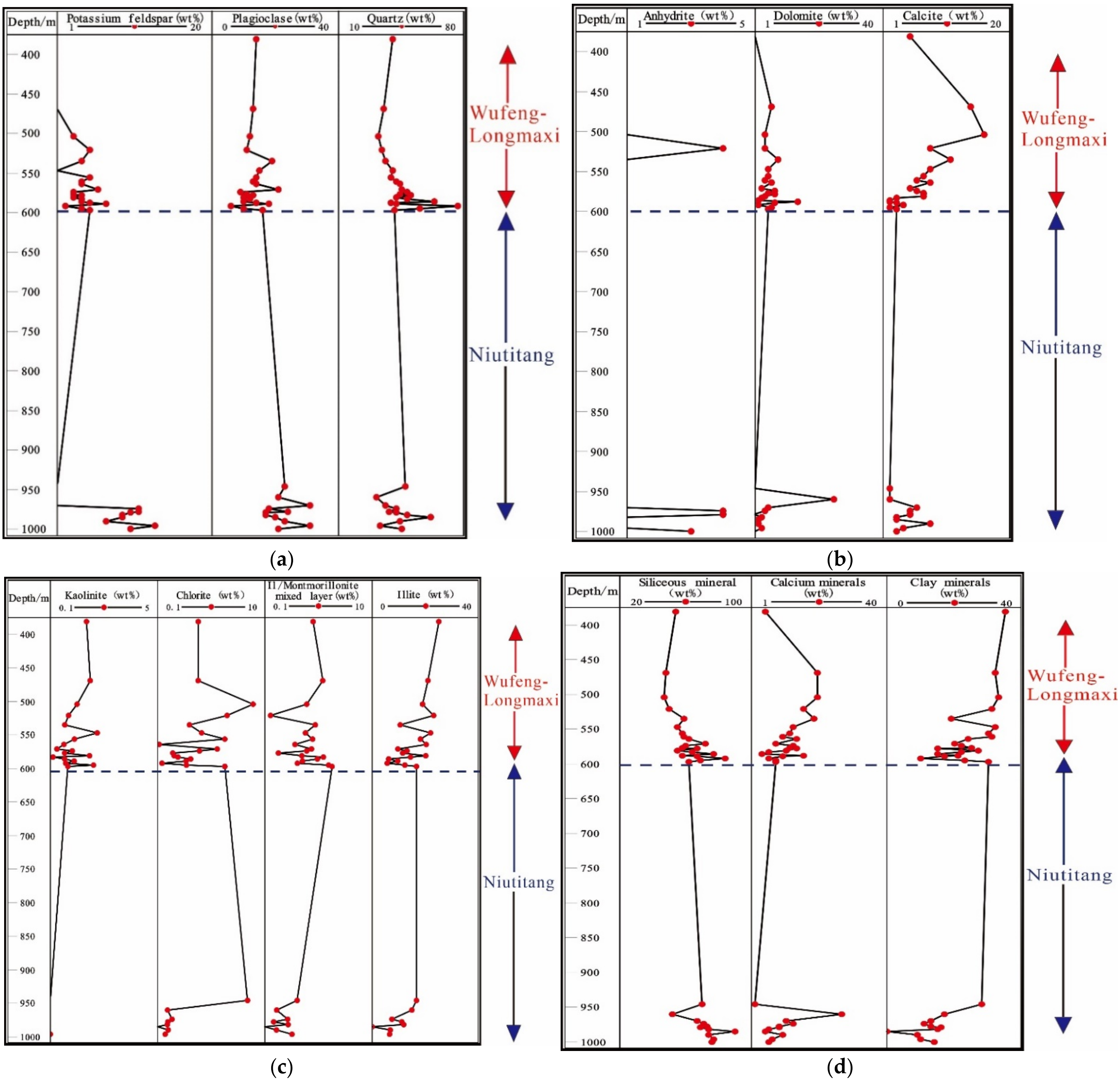

Figure 3. Mineral composition characteristics of the Wufeng-Longmaxi and Niutitang Formations in northern Guizhou Province. (**a**) Siliceous mineral composition (quartz, plagioclase, and potassium feldspar); (**b**) calcareous mineral composition (calcite, dolomite, and anhydrite); (**c**) clay mineral composition (kaolinite, chlorite, illite, and il/montmorillonite mixed layer); (**d**) total mineral composition (siliceous minerals, calcium minerals, and clay minerals).

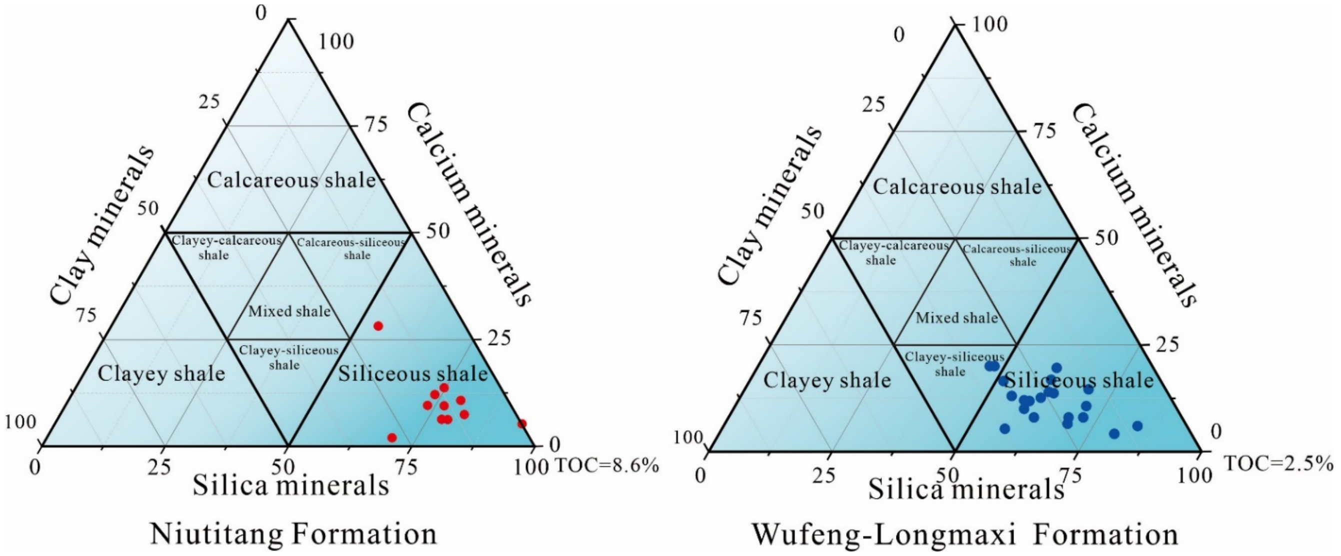

Figure 4. Lithofacies distribution characteristics of samples between the Wufeng-Longmaxi Formation and the Niutitang Formation in northern Guizhou Province [41].

4.3. Pore Types

Pores cannot exist as independent entities and must occur in a solid framework in the shale matrix [42]. The pore types and the characteristics of pore space can be determined by scanning electron microscopy, which can observe the morphology and size characteristics of different pores in shale reservoirs. The FIB-SEM results show that nano–microscale pores are developed in the Wufeng-Longmaxi and Niutitang Formations.

There are numerous types of shale pores, including organic matter pores, brittle mineral pores, and clay mineral pores. The shale reservoirs of the Wufeng-Longmaxi Formation with higher silica content have developed more organic matter pores than the Niutitang Formation. The shale of the Niutitang Formation has reached the over-mature stage, and the form of organic matter is uncertain, which is filled with mineral particles and fractures (Figure 5H). It is worth noting that organic matter is mostly in contact with secondary cement, such as secondary mineral particle gaps and clay mineral plates (Figure 5K,L). The organic matter pores in the Niutitang Formation are oval, gneisses, and irregular polygons, showing strong heterogeneity (Figure 5K,L). The organic matter of the Wufeng-Longmaxi Formation has reached a high-maturity stage, with regular shapes observed under a scanning electron microscope, and the organic matter pores are distributed continuously and densely like honeycomb (Figure 5J). The formation process of organic matter pores has the advantages of methane adsorption and storage, which play a positive role in the generation of free gas and adsorbed gas [43].

The clay mineral intergranular pores of the Niutitang Formation were formed by contraction and crystal accumulation (Figure 5E,F), and they were partially filled with pyrite (Figure 5E). The development of mylonitic mineral intergranular pores and fractures effectively improved the porosity and permeability of Wufeng-Longmaxi shale reservoirs (Figure 5D) [44]. The intergranular pores were filled with organic matter and argillaceous minerals, and only microcracks were found around the edges of the residual particles (Figure 5I). There are dissolution pores in calcite grains of the Wufeng-Longmaxi Formation, which are evenly distributed and nearly round in shape (Figure 5C).

Both the Wufeng-Longmaxi and Niutitang Formations have developed clay mineral intergranular microfractures (Figure 5A,B,G), which are linear or strip-shaped and about 15~55 µm in length.

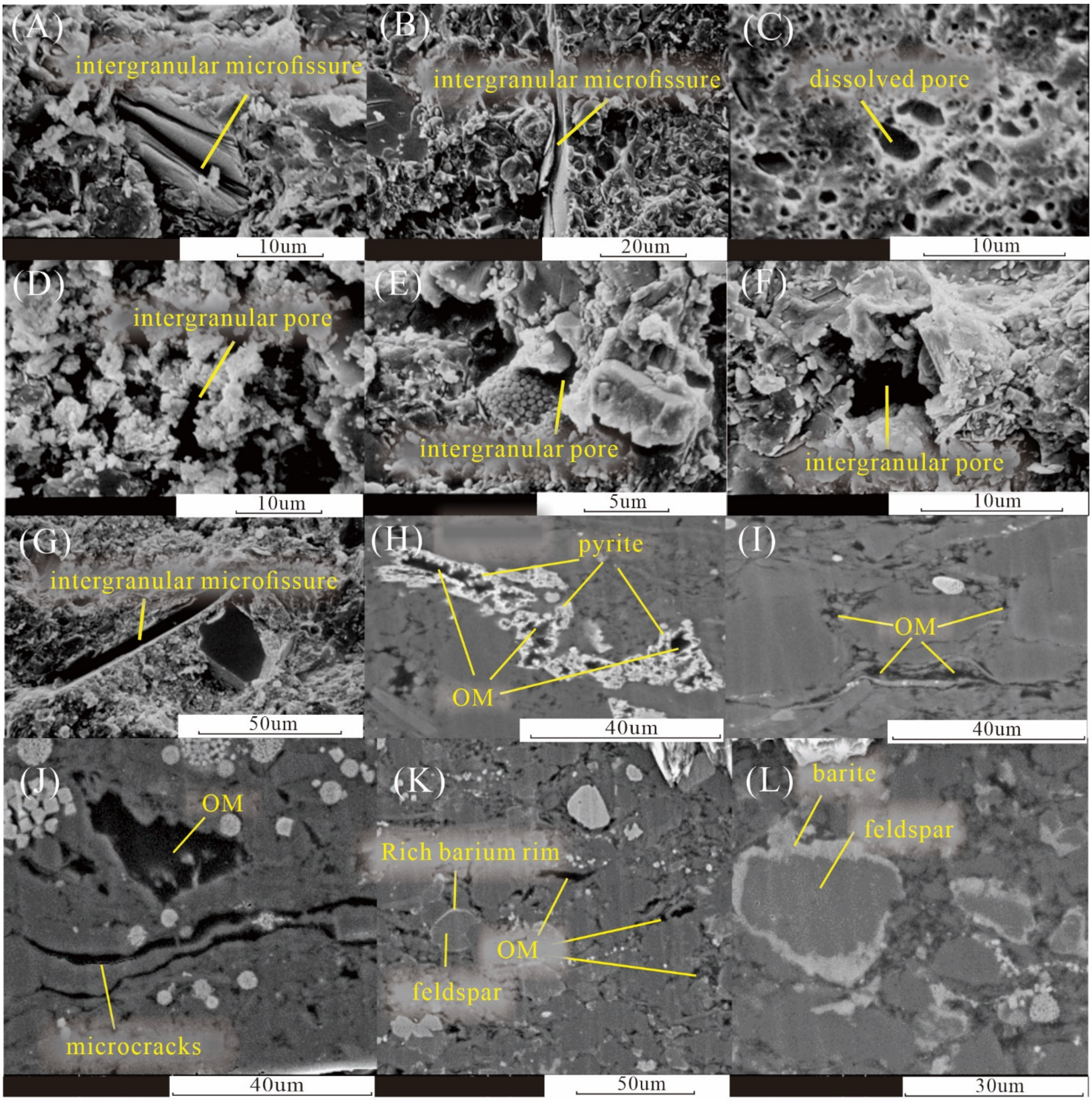

Figure 5. Scanning electron microscopy characteristics of pores in shales of the Wufeng-Longmaxi and Niutitang Formations in northern Guizhou Province. (**A**,**B**,**G**) Intergranular microfractures of clay minerals, (**C**) calcite dissolution pores, (**D**) intergranular pores of mylonitic mineral grains, (**E**) intergranular pores of clay minerals partially filled with pyrite, (**F**) intergranular pores of clay minerals, (**H**) organic matter filled with pyrite, (**I**) intergranular pores plugged by organic matter and mud, (**J**) organic matter pores developed within organic matter, (**K**) organic matter uniformly distributed in intergranular micropores, and (**L**) feldspar particles surrounded by barite.

The feldspar particles are generally surrounded by barite and barium-rich minerals, which may have been derived from volcanic ash in the Niutitang Formation (Figure 5K,L).

4.4. Microscopic Pore Structure Characteristics

Mercury intrusion and low-pressure N_2 adsorption experiments were applied to quantitatively characterize the structures of macropores and mesopores.

4.4.1. Pore Structure from High-Pressure Mercury Intrusion

The mercury intrusion curve can reflect the degree of pore development and the filtration properties of the shale reservoir. Capillary pressure curves of the Wufeng-Longmaxi and Niutitang Formation samples in northern Guizhou Province were established by high-pressure mercury intrusion (Figure 6). For samples from the Wufeng-Longmaxi Formation, the amount of mercury was low when the capillary pressure of the DY1-23 sample was between 0.1838 and 11.6667 MPa, indicating that the development of macropores ranging from 0.063 to 4 μm is poor. When the capillary pressure was higher than 18.375 MPa and between 0.0117 and 0.0294 MPa, the mercury rapidly increased by more than 75%, indicating that pores with pore sizes of 0.006~0.04 μm and 25~63 μm developed. More mesopores ensure the high adsorption and accumulation capacity of the shale reservoirs. As for the pore-throat distribution, the relative offset between mercury intake and mercury withdrawal was more pronounced, indicating the existence of ink-bottle pores in shale, which is conducive to the adsorption of shale gas.

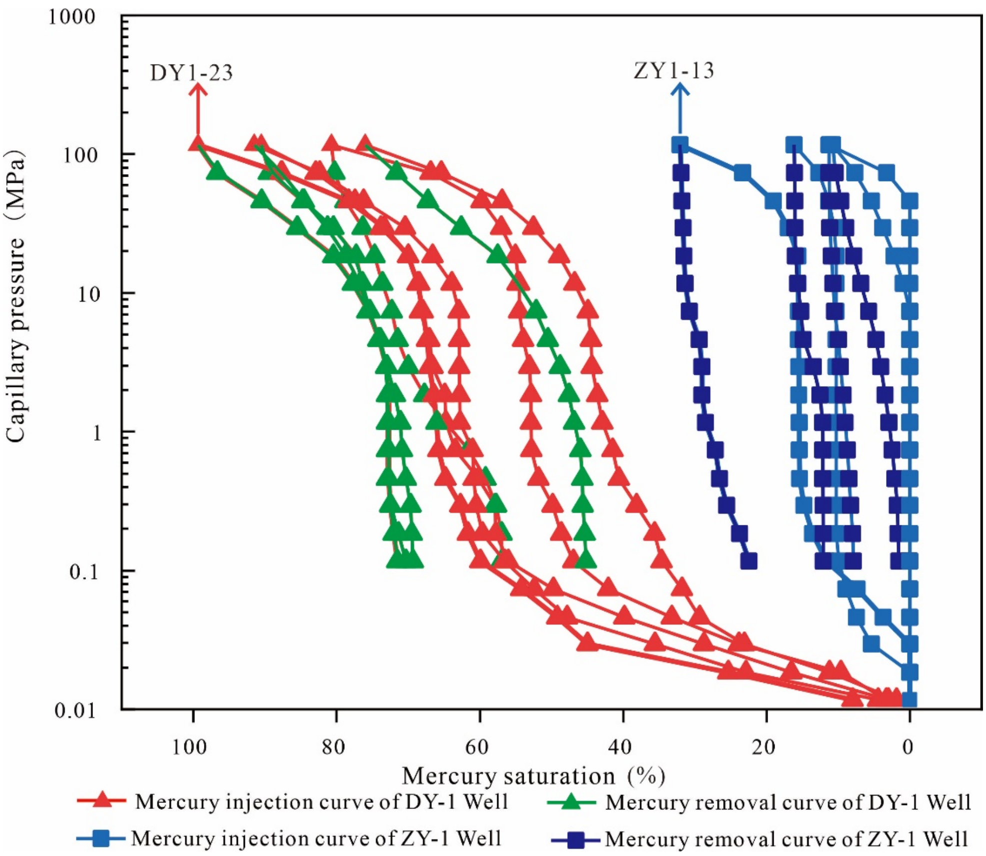

Figure 6. Capillary pressure curves of the Wufeng-Longmaxi Formation and Niutitang Formation shales in northern Guizhou Province based on high-pressure mercury intrusion.

When the capillary pressure of the ZY1-13 sample was 0.735~18.375 MPa, the amount of mercury was low, indicating that the development of macropores ranging from 0.04 to 1 μm is poor. There was no mercury intrusion between 0.0117 and 0.0294 MPa, which shows that it did not develop macropores with sizes between 25 and 63 μm. Once the capillary pressure was higher than 29.4 MPa and in the range of 0.0459 to 0.1167 MPa, the amount of mercury increased rapidly by more than 25%, indicating that pores with pore sizes of 0.006~0.025 μm and 6.3~16 μm developed. The volume difference between mercury intake and mercury withdrawal shows that the shale reservoir mainly developed open tapered holes, indicating that the shale gas tends to escape, which destroys the preservation conditions of shale gas.

The pore structure parameters of the Wufeng-Longmaxi and Niutitang shales in northern Guizhou Province were calculated based on high-pressure mercury intrusion (Table 5). The macropore specific surface area of the Wufeng-Longmaxi and Niutitang Formations ranges from 4.51 to 190.96 m^2/g (average of 84.23 m^2/g) and 330.80 to 3498.24 m^2/g (average of 1387.44 m^2/g), respectively. As for the pore volume, it ranges from 0.08 to 0.17 mL/g, with an average of 0.13 mL/g in Wufeng-Longmaxi shale and 0.05 to 0.14 mL/g (average of 0.08 mL/g) in Niutitang shale. The Hg porosity ranges from 0.84 to 1.71% (average of 1.29%) and 0.48 to 1.48% (average of 0.92%), respectively. The average throat radius ranges from 20.45 to 27.24 μm (average of 23.3 μm) and 0.01 to 15.90 μm (average of 5.71 μm), respectively.

Table 5. Pore structure parameters of shale in the Wufeng-Longmaxi and Niutitang Formations in northern Guizhou Province based on the high-pressure mercury intrusion method.

Well	Sample ID	Formation	Depth/m	Pore Volume/cm^3	Specific Surface Area/(m^2/g)	Hg Porosity/%	Average Throat Radius/μm
DY-1	DY1-2	Wufeng-Longmaxi	545.99	0.08	9.69	1.71	21.04
	DY1-6		554.84	0.17	190.96	1.46	22.40
	DY1-9		559.51	0.15	58.51	1.18	20.45
	DY1-16		572.15	0.1	4.51	0.84	25.38
	DY1-23		586.15	0.15	157.46	1.27	27.24
ZY-1	ZY1-4	Niutitang	958.25	0.05	330.80	1.48	0.03
	ZY1-13		974.30	0.07	856.26	0.48	6.91
	ZY1-25		987.30	0.14	3498.24	1.16	15.90
	ZY1-36		1002.73	0.05	864.45	0.56	0.01

4.4.2. Mesopore Structure Characterization Based on N_2 Adsorption

Low-pressure N_2 adsorption was used to quantify mesopore (2 nm < d < 50 nm) structures. Due to capillary condensation, the adsorption–desorption isotherms separate, which forms a hysteresis loop (Figure 7) within a relative pressure (P/P_0, P is the balance pressure, and P_0 is the saturation pressure) greater than 0.42. When P/P_0 is close to 1, the adsorption and desorption isotherms tend to coincide, indicating that the hysteresis loop has a tendency to close. According to DeBoer's theory, the Wufeng-Longmaxi shale reservoir is dominated by ink-bottle pores, and the Niutitang shale contains more open tapered wall holes.

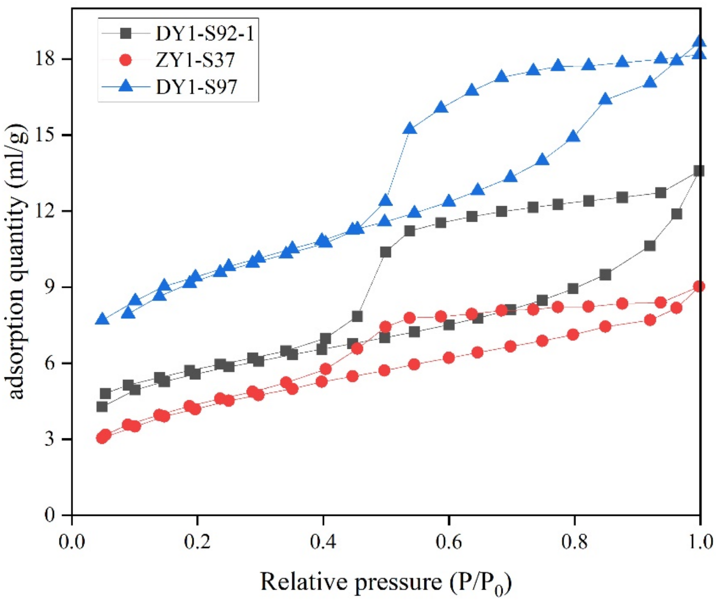

Figure 7. Nitrogen adsorption–desorption curves for the Wufeng-Longmaxi and Niutitang Formation shales in northern Guizhou Province.

The pore structure parameters of shale in the Wufeng-Longmaxi Formation and Niutitang Formation were calculated based on N_2 adsorption (Table 6). The mesopore specific surface area of the Wufeng-Longmaxi and Niutitang Formations ranges from 9.968 to 15.237 m^2/g (average of 13.5 m^2/g) and 3.357 to 12.97 m^2/g (average of 7.5 m^2/g), respectively, and the mesoporous volume ranges from 0.013 to 0.035 mL/g (average of 0.018 mL/g) and 0.008 to 0.03 mL/g (average of 0.016 mL/g), respectively. The Wufeng-Longmaxi and Niutitang shales span an average pore size range of approximately 3.62 to 4.68 nm (average of 3.92 nm) and 3.59 to 6.28 nm (average of 4.12 nm).

Table 6. Pore structure parameters of shale in the Wufeng-Longmaxi and Niutitang Formations in northern Guizhou Province based on the N_2 adsorption method.

Well	Sample ID	Formation	Depth/m	Specific Surface Area/(m^2/g)	Pore Volume/(mL/g)	Average Pore Diameter/nm
DY-1	DY1-S61	Wufeng-Longmaxi	564.300	15.237	0.014	3.623
	DY1-S71		573.500	13.083	0.015	3.824
	DY1-18		576.630	14.931	0.035	3.773
	DY1-S77		577.700	13.678	0.016	3.811
	DY1-S82		580.700	14.172	0.017	4.683
	DY1-S106		597.150	9.968	0.013	3.811
ZY-1	ZY1-11	Niutitang	969.500	3.357	0.030	6.282
	ZY1-S37		970.675	7.769	0.009	3.731
	ZY1-17		979.300	6.260	0.019	3.702
	ZY1-S53		984.905	8.608	0.008	3.589
	ZY1-S73		999.250	12.970	0.012	3.733

4.5. Shale Gas Content

The shale gas content of the Wufeng-Longmaxi and Niutitang Formations was tested (Table 7). The gas content of the Wufeng-Longmaxi and Niutitang shales ranges from 0.04 to 2.69 m^3/t (average of 1.48 m^3/t) and 0.9 to 2.05 m^3/t (average of 1.28 m^3/t), respectively.

Table 7. The gas content of shale reservoirs in the Wufeng-Longmaxi and Niutitang Formations in northern Guizhou Province.

Well	Formation	Depth/m	Gas Content/(m^3/t)
DY-1	Wufeng-Longmaxi	553.56	1.84
		559.20	0.04
		580.90	0.07
		589.90	2.20
		592.70	2.69
		595.80	2.03
ZY-1	Niutitang	1003.31	1.36
		1006.16	1.28
		1008.05	1.20
		1010.05	1.18
		1010.71	1.09
		1011.51	1.37
		1013.91	0.90
		1018.35	0.97
		1018.89	2.05
		1020.34	1.11
		1022.01	1.56
		1022.71	1.30

The shale gas components of the above two formations in northern Guizhou were tested (Table 8). The CH_4 content of the Wufeng-Longmaxi and Niutitang Formations ranges from 47.22 to 88.91% (average of 71.5%) and 5.27 to 8.09% (average of 6.68%), and the N_2 content ranges from 7.56 to 40.01% (average of 21.18%) and 57.32 to 65.42% (average of 61.37%), which may be related to strong tectonic uplift, magmatic activity, and upwelling ocean current during the deposition period of the Niutitang Formation.

Table 8. Gas components of the Wufeng-Longmaxi and Niutitang Formations in northern Guizhou Province.

Well	Formation	Depth/m	CH_4/vol	N_2/vol	O_2/vol	CO_2/vol	C_2H_6/vol	C_3H_8/vol	H_2/vol
DY-1	Wufeng-Longmaxi	589.90	78.36	15.97	4.37	0.87	0.43	0	-
		592.70	88.91	7.56	2.39	0.68	0.46	0	-
		595.80	47.22	40.01	10.18	1.04	1.55	0	-
ZY-1	Niutitang	1011.51	5.27	57.32	0.00	0.43	0.01	0.00	36.98
		1022.71	8.09	65.42	0.00	1.77	0.01	0.00	24.70

5. Discussion

5.1. Differential Pore Development Characteristics

5.1.1. Differential Organic Matter Pore Development Characteristics

It has been found that organic matter does not exist alone but usually exists together with clay minerals, quartz, carbonate minerals, pyrite, etc. [45]. As we can see, the organic matter in Figure 8a,b developed together with pyrite, and the organic matter in Figure 8c developed around feldspar. Pore morphology parameters, such as plane porosity, pore diameter, roundness, convex degree, elongation, and the fractal dimension of organic pores, were extracted by IPP technology (Figure 8). Plane porosity refers to the ratio of the pore area to the matrix area, which reflects the overall development of pores. The roundness, elongation, and fractal dimension of organic pores all reflect the deformation degree of the pores, and the convex degree reflects the roughness of pores. At present, according to research, micro-CT 3D reconstruction is widely used in 3D shale reservoir space research. With the two-dimensional profile, we can more vividly describe the change regularity of the pore morphology of micro–nanopores in the thermal evolution process by using pore morphology parameters to reflect their development degree: surface porosity, roundness, elongation, and fractal dimension. For the quantitative description of the degree of pores in different evolution stages of shale, it is difficult to achieve an accurate and multi-directional description of the two-dimensional plane in three-dimensional space due to the heterogeneity and interference factors of the three-dimensional space description. Therefore, in the study of pore structure evolution, studying the two-dimensional plane is more advantageous.

As is shown in Figure 8, the morphological parameters of organic matter pores were extracted from one sample from the Wufeng-Longmaxi Formation, namely, DY1-S86, and from two samples from the Niutitang Formation, namely, ZY1-S39 and ZY1-S74. It is considered that type I kerogen mainly produces intermediate macromolecules and shrinks to produce marginal pores of organic matter due to the “depolymerization” reaction, while type III kerogen mainly produces internal pores of organic matter due to the main “Parallel defunctionalization” reaction. It is worth noting that a large number of organic matter marginal pores have developed in highly mature shale reservoirs in the northern Guizhou area (Figure 8b,c), and the storage space provided by the organic matter marginal pores is greater than that provided by the organic matter internal pores [46]. Based on the IPP extraction, the morphological parameters of organic matter pores were calculated (Table 9). From samples of the Wufeng-Longmaxi to Niutitang Formations, the plane porosity of the organic matter pores of the samples gradually decreases (Table 9), which indicates that the organic matter pores become less developed. The average pore size and pore size distribution range continue to increase, indicating an increase in the proportion of relatively large organic pores and an increase in the heterogeneity of organic pores (Table 9). The roundness and convex degree gradually increase (Table 9), indicating not only that the organic pore morphology becomes more irregular but also that the pore walls become rougher; the elongation increases significantly (Table 9), indicating that the proportion of narrow organic matter pores increases significantly. The fractal dimension of organic matter pores increases (Table 9), indicating that the pore morphology becomes more complex and the structural heterogeneity increases [46].

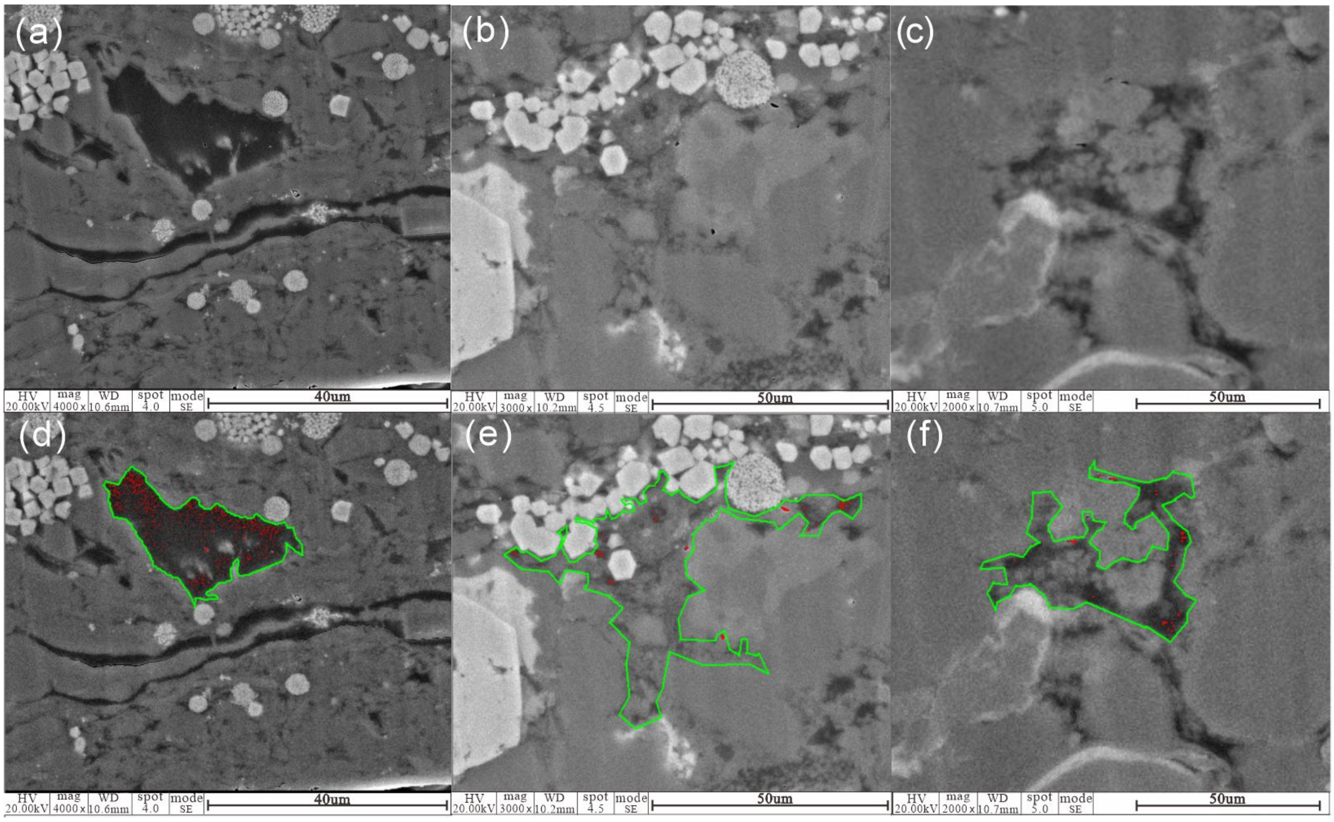

Figure 8. Organic matter pores in the shales of the Wufeng-Longmaxi Formation and Niutitang Formation in northern Guizhou Province. (**a**) DY1-S86 of the Wufeng-Longmaxi Formation; (**b**) ZY1-S39 of the Niutitang Formation; (**c**) ZY1-S74 of the Niutitang Formation; (**d**) DY1-S86 organic matter pore extraction of the Wufeng-Longmaxi Formation; (**e**) ZY1-S39 organic matter pore extraction of the Niutitang Formation; (**f**) ZY1-S74 organic matter pore extraction of the Niutitang Formation.

Table 9. Organic matter pore morphology parameters of shale in the Wufeng-Longmaxi and Niutitang Formations in northern Guizhou Province.

Sample ID	Formation	Depth/m	Plane Porosity	Pore Diameter$_{max}$/nm	Pore Diameter$_{min}$/nm	Pore Diameter AVG/nm	Roundness	Convex Degree	Elongation	Fractal Dimension
DY1-S86	Wufeng-Longmaxi	583.1	0.026	85.559	74.188	79.873	5.007	15.941	1.554	1.151
ZY1-S39	Niutitang	974.64	0.007	168.873	115.138	142.006	7.298	19.030	2.057	1.184
ZY1-S74	Niutitang	1000.05	0.011	227.897	157.464	192.681	8.747	46.964	1.778	1.199

The organic matter of the Wufeng-Longmaxi Formation in northern Guizhou Province is at a high thermal evolutionary level, and a large amount of gas production at this stage promoted the development of organic matter pore space. The Niutitang Formation is at an over-mature stage, and the hydrocarbon generation capacity of organic matter has declined, while the deeper burial depth of the Niutitang Formation has resulted in stronger mechanical compaction. The combined effect of the above two factors is the main reason for the relatively poor development of organic pore space in Niutitang shale [47–50].

Compared with the Niutitang Formation, the organic pore morphology of Wufeng-Longmaxi shale is more regular, indicating that the organic pores in the Wufeng-Longmaxi Formation are less deformed. This is due to the support of a rigid mineral skeleton that provides good protection to the organic matter pores, which is confirmed in this paper by the significantly higher content of quartz, pyrite, and carbonate minerals in the Wufeng-Longmaxi Formation compared to the Niutitang Formation. These effective support and protective effects result in better gas preservation in Wufeng-Longmaxi shale.

5.1.2. Differential Intergranular Pore and Microfracture Development Characteristics

The plane porosity of intergranular pores from Wufeng-Longmaxi to Niutitang Formations was extracted by IPP technology (Figure 9). From the samples in the Wufeng-Longmaxi to Niutitang Formations, the plane porosity of intergranular pores gradually decreases, indicating that the intergranular pores become less developed (Table 10).

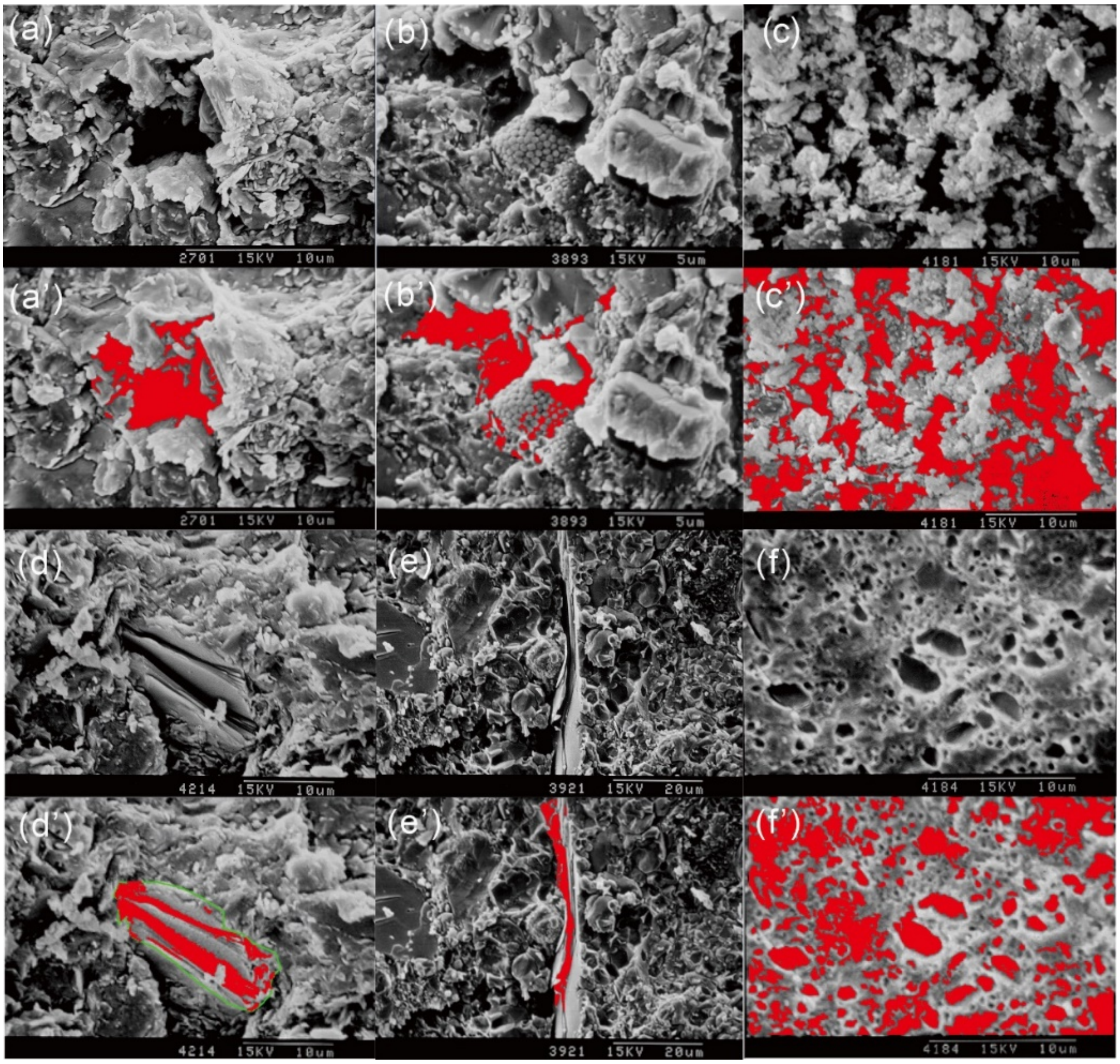

Figure 9. Extraction of pore features from shales of the Wufeng-Longmaxi and Niutitang Formations in Guizhou Province. (**a**–**c**) The original images of intergranular pores corresponding to "a′ to c′"; (**a′**–**c′**) Extraction of intergranular pore features, (**d**,**e**) The original images of intergranular microfractures corresponding to "d′ to e′"; (**d′**,**e′**) extraction of intergranular microfracture features; (**f**) The original images of dissolution pores corresponding to "f"; (**f′**) extraction of dissolution pore features.

Quartz itself has no pores, but quartz particles have good compaction resistance, which can prevent the pores from being damaged by compaction, and quartz is mostly associated with clay minerals, which have a good support effect on the pores in shale reservoirs. The quartz content in the Wufeng-Longmaxi Formation and Niutitang Formation shale reservoirs are almost the same (average values are 44.5% and 42.5%, respectively), but the content of clay minerals associated with quartz of the Wufeng-Longmaxi Formation is higher than that of the Niutitang Formation (average values are 24.5 and 13.3%, respectively), indicating the stronger support of a mineral skeleton that provides good protection to the intergranular pores. The symbiosis of quartz and clay minerals can form a good supporting skeleton. The increase in clay minerals promotes the development of micropores and mesopores, and compaction causes gradual densification of the reservoir, which is a destination layer, so it is more conducive to the preservation of micropores and mesopores in terms of shale gas preservation. The deeper burial depth of Niutitang shale resulted in stronger mechanical compaction, which resulted in greater damage to the protective effect of intergranular pores with less clay mineral content at the same time. The above two factors together became the main control factors for the relatively better development and preservation ability of intergranular pores in the target interval of Wufeng-Longmaxi shale.

Table 10. The plane porosity of the intergranular pores in the Wufeng-Longmaxi Formation and Niutitang Formation.

Well	Sample ID	Formation	Depth/m	Plane Porosity/%
DY-1	DY1-S61	Wufeng-Longmaxi	564.3	4.10
	DY1-S71		573.5	7.10
	DY1-18		576.63	6.70
	DY1-S77		577.7	9.30
	DY1-S82		580.7	7.20
ZY-1	ZY1-S21	Niutitang	954.665	6.80
	ZY1-S29		964.07	3.04
	ZY1-S36		969.965	3.70
	ZY1-S53		984.905	5.90
	ZY1-S62		992.45	6.40
	ZY1-S73		999.25	3.80

Natural microfractures have developed in Wufeng-Longmaxi and Niutitang shales. As far as we know, natural fractures are fractures formed under the action of extrusion or abnormally high pressure in the long-term geological process. The cross-section of natural fractures is relatively smooth, and the extension of the microfractures is limited. In addition, most of the mineral particles, such as quartz and feldspar, are cut through. In most cases, minerals (quartz, etc.) are filled when observed under the microscope (as shown in Figure 10). From the samples of the Wufeng-Longmaxi shale to Niutitang shale, the microfracture opening of the samples gradually decreases (microfracture openings are reduced from 4031.3 nm to 1990.1 nm), indicating that the intergranular microfractures become less developed (Figure 10).

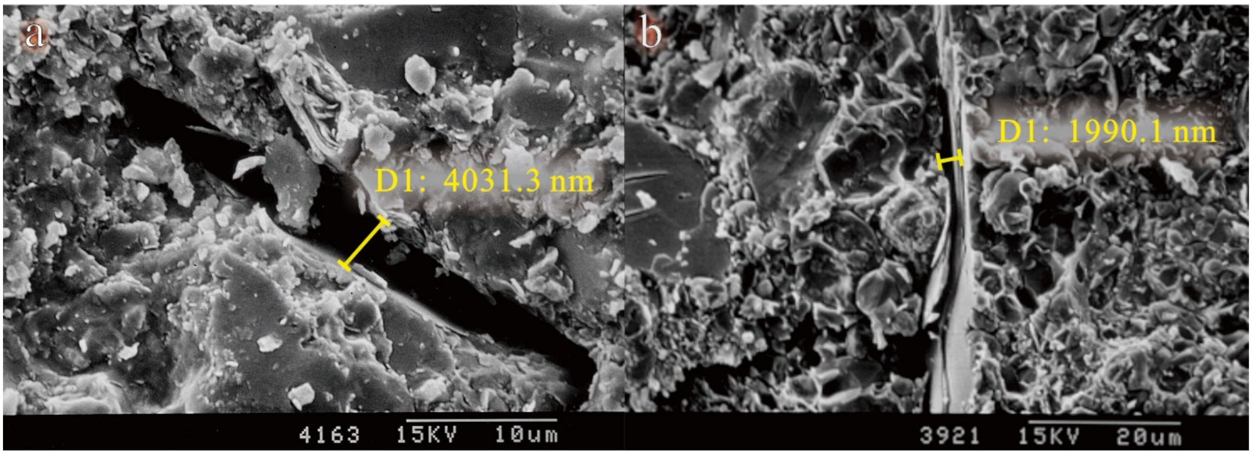

Figure 10. Microfractures in shale reservoirs of the Wufeng-Longmaxi Formation and Niutitang Formation in northern Guizhou Province. (**a**) DY1-S77 microfracture; (**b**) ZY1-S87 microfracture.

The TOC of the Wufeng-Longmaxi Formation is generally higher, and the part with more enriched organic matter corresponds to the stress-weakened surface, which more readily develops microfractures. The quartz contents of Wufeng-Longmaxi shale are higher, indicating greater brittleness. The organic matter in the Wufeng-Longmaxi shale is in the evolutionary stage of high maturity and at the peak of gas production. A large amount of gas generation in this stage promotes the conformation of abnormal reservoir pressure [51]. However, the Niutitang Formation is in the over-mature stage, and its hydrocarbon generation capacity has decreased. The above factors together become the main control factors for the relatively better development of microfractures in Wufeng-Longmaxi shale.

5.2. Quantitative Characterization of Differential Behaviors in Pore Structure Features

The average pore volume of the shale samples in the Wufeng-Longmaxi Formation is greater than that of the Niutitang Formation in northern Guizhou Province (Tables 5 and 6), as are the mercury porosity and the average throat radius, while the average specific surface area of the macropores of Wufeng-Longmaxi shale is much smaller than that of Niutitang shale. The multi-scale pore size distributions from the Wufeng-Longmaxi and Niutitang Formations were established (Figure 11). The dominant pore sizes of macropores in the Wufeng-Longmaxi Formation mainly range from 16 to 25 μm, 25 to 40 μm, and 40 to 63 μm, whereas the dominant pore sizes of macropores of the Niutitang Formation are smaller, with the distribution mainly ranging from 4 to 6.3 μm, 6.3 to 10 μm, and 10 to 16 μm, indicating that the dominant pore size of macropores in Wufeng-Longmaxi Formation shale is larger than that in Niutitang shale. The Wufeng-Longmaxi shale has higher-frequency peaks of mercury intake saturation, indicating that it is more developed with ink-bottle pores (Figure 11a). The pore volume of mesopores in Wufeng-Longmaxi shale is mainly contributed to by pore sizes around 3.8 nm, while the pore volume of mesopores in the Niutitang Formation is mainly contributed to by pore sizes around 3.6 nm, and the mesopores of both contribute equally to the pore volume (Figure 11b). The macropore specific surface area in Wufeng-Longmaxi shale is much smaller than that in Niutitang shale, indicating that macropores in organic matter provide the main specific surface area (Table 5). The TOC of Niutitang shale is much larger than that of Wufeng-Longmaxi shale (Table 1), so the former has a larger specific surface area than the latter. As the organic matter in Wufeng-Longmaxi shale is at a high-maturity evolutionary stage and undergoing massive shale gas generation, the reservoir porosity also increases as a result, whereas Niutitang shale is already in the over-mature stage (Ro > 2.0), and the porosity tends to decrease with increasing organic matter maturity. Therefore, the porosity in the Wufeng-Longmaxi shale reservoir is greater than that in the Niutitang shale reservoir.

The Wufeng-Longmaxi shale in northern Guizhou Province has developed intergranular pores with clay minerals, microcracks, and calcite grains from a large number of nanoscale dissolution pores due to dissolution (Figure 5). The Niutitang Formation shale in northern Guizhou Province has developed microscale intergranular pores, accompanied by the presence of pyrite aggregates, and the reservoir has also developed microscale intergranular pores filled with clay minerals and nanoscale microfissures between clay mineral flakes (Figure 5).

Based on our comprehensive analysis, the influencing factors of the evolution of the shale reservoir space in the Niutitang Formation in the complex structural area of northern Guizhou are relatively complex, and the correlation between the organic geochemistry, mineral composition, and the evolution of the pore structure of the Niutitang Formation is much weaker than that of the Wufeng-Longmaxi Formation, whose correlation coefficients of Ro, TOC, clay mineral content, and plane porosity are 0.0234, 0.0005, and 0.1455, respectively. As a result, it is not typical of the study in Niutitang shale. This may be related to the high degree of maturity of the Niutitang Formation, which leads to the collapse of pores to a large extent and a worse correlation between its organic geochemistry, mineral composition, and pore structure.

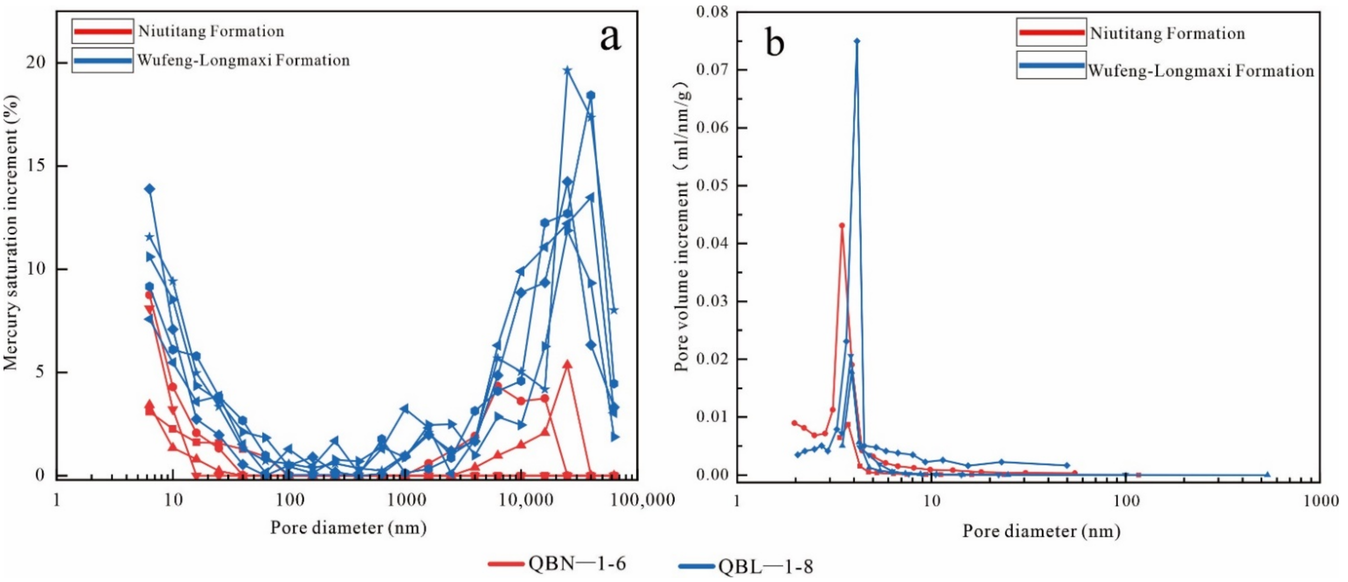

Figure 11. Multi-scale pore size distribution curves from the Wufeng-Longmaxi and Niutitang Formations. (**a**) Pore size distribution calculated by high pressure mercury; (**b**) Pore size distribution calculated by low temperature nitrogen adsorption.

The plane porosity was correlated with Ro, clay mineral content, and TOC of the Wufeng-Longmaxi shale samples, indicating that the above factors control the pore structure of Wufeng-Longmaxi shale (Figure 12a–c). The mesopore specific surface area was positively correlated with TOC in both Wufeng-Longmaxi and Niutitang shales, and the correlation between them was higher in Wufeng-Longmaxi shale, indicating that TOC control over the mesopore specific surface area is more pronounced in Wufeng-Longmaxi shale (Figure 12d).

5.3. Main Controlling Factors and Differential Mechanisms of Shale Gas Reservoir

There are obvious differences in the pore types and pore structure parameters of shale reservoirs between the Wufeng-Longmaxi and Niutitang shales in northern Guizhou Province. The main controlling factors for this variability include lithofacies categories, the degree of the thermal evolution of organic matter, and tectonic preservation conditions.

5.3.1. Lithofacies Categories

Lithofacies categories are closely related to the depositional environment, mineral composition, organic matter abundance, rock mechanical properties, and pore structure. Siliceous shale, clayey shale, calcareous shale, mixed clayey–siliceous shale, mixed clayey–calcareous shale, and mixed calcareous–siliceous shale were classified according to the mineral content characteristics of the shales in the two sets of strata (Table 4).

Most of the samples from Wufeng-Longmaxi shale belong to the siliceous shale phase, while a minority belong to the mixed clayey–siliceous shale phase, with a slightly higher carbonate mineral content than that of the Niutitang Formation (Figure 3b). The samples are mainly composed of quartz, feldspar, and clay minerals, with pyrite seen locally, and some of the pyrite grains are internally filled with organic matter (Figure 5A,E), and horizontal lamination has developed. The clay mineral content of the samples (between 10 and 35%) has caused the intergranular pores associated with the clay minerals to be more developed (Figure 5A,B), and the organic pores are developed. During the depositional period of Wufeng-Longmaxi shale, the water bodies were shallow and occluded, with weak hydrodynamics, anoxic and reducing water environments, and warm and humid paleoclimate, which promoted the formation and dissolution of carbonate minerals, prompting the development of more mineral dissolution pores in Wufeng-Longmaxi shale (Figure 5C) and also promoting the formation of more fine bottle-neck ink-bottle pores in the reservoir to further enhance the adsorption capacity of the reservoir for shale gas.

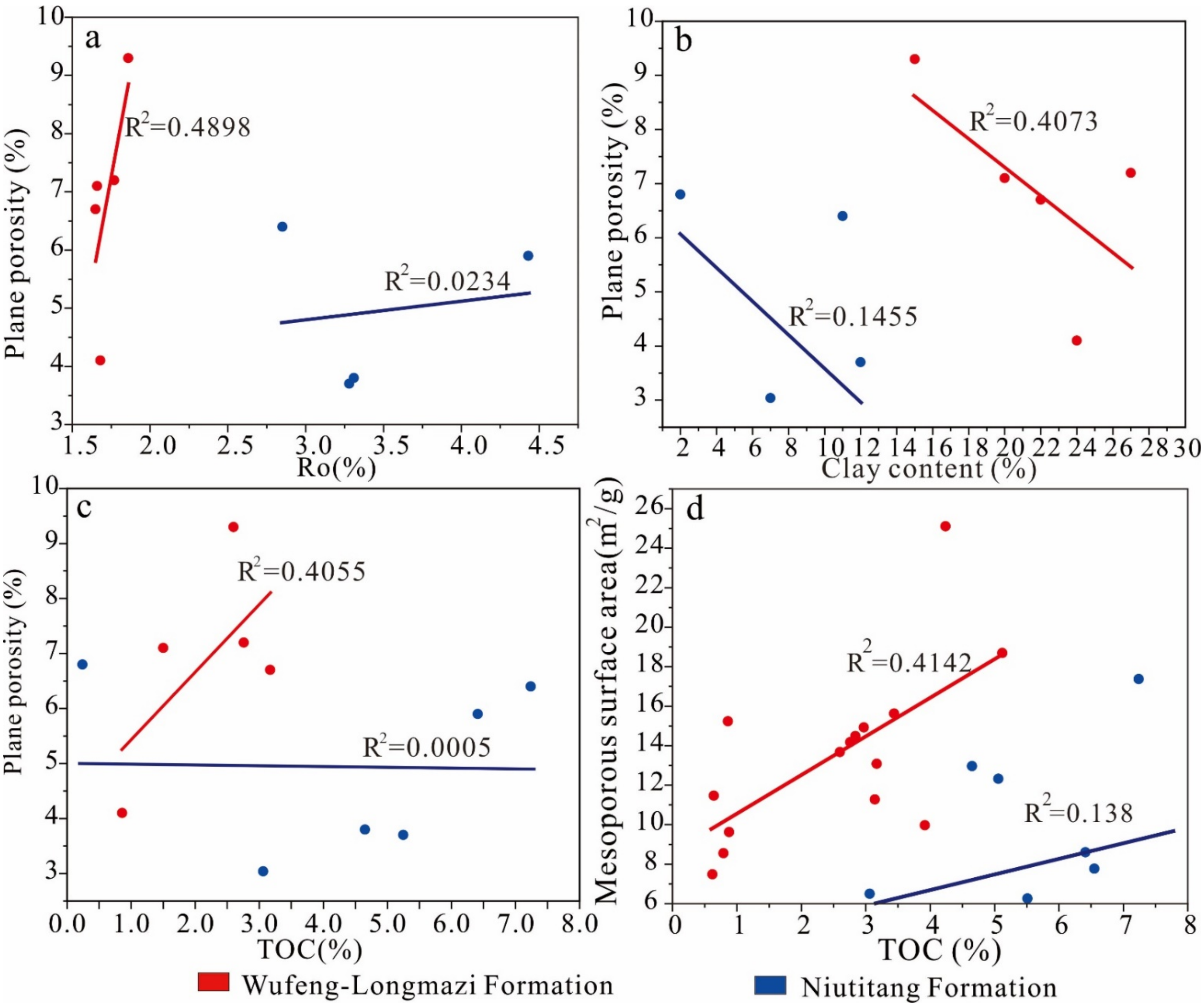

Figure 12. Correlation between Ro, clay content, TOC, and pore structure parameters. (**a**) Correlation map between Ro and Plane porosity of Wufeng-Longmaxi and Niutitang Formations; (**b**) Correlation map between Clay content and Plane porosity of Wufeng-Longmaxi and Niutitang Formations; (**c**) Correlation map between TOC and Plane porosity of Wufeng-Longmaxi and Niutitang Formations; (**d**) Correlation map between TOC and Mesoporous surface area of Wufeng-Longmaxi and Niutitang Formations.

The samples from Niutitang shale all belong to the siliceous shale phase (Figure 4), with siliceous content ranging from 52 to 90% (Figure 3d) and generally low content of calcareous and clay minerals. The lower porosity is due to the compaction and cementation of shale under the pressure of the overlying formations, which destroyed the microscopic pores and reduced the porosity. In addition, the Niutitang Formation has developed horizontal grain layers and is thicker than the Wufeng-Longmaxi Formation with high-angle fractures, which may be due to the high pressure of the overlying formations, the brittle nature of the siliceous shale, and the formation of high-angle fractures.

The occurrence of clay minerals in shale reservoirs also has a controlling effect on pore development. As Ro increases, the diagenesis of Niutitang Formation shale in northern Guizhou Province strengthens accordingly, while the content of montmorillonite, which contributes more surface area to the clay minerals, gradually decreases and is successively converted to illite or chlorite, during which the specific surface area and pore volume of the clay minerals are greatly reduced.

5.3.2. Degree of Thermal Evolution of Organic Matter

The degree of thermal evolution also affects the organic matter pore structure [52], and too low or too high of a thermal evolution degree is detrimental to the development of organic matter pores. The plane porosity of the Wufeng-Longmaxi Formation samples increases with increasing reflectivity (Figure 12a), indicating that increasing reflectivity promotes the development of organic pores, and the organic matter of the Wufeng-Longmaxi Formation shales as a whole is at a high-maturity stage, mostly near the peak of gas production, producing large amounts of oil fracturing gas and developing a large number of organic pores. In addition, the acidic fluids produced during the pyrolysis of organic matter caused the dissolution of carbonate minerals, leading to the development of a lot of dissolution pores in the reservoir (Figure 5C). The organic matter of the Niutitang Formation shale has entered the over-maturation stage of evolution, with Ro generally greater than 2.5%, and is in the late over-maturation and late diagenesis, low metamorphic stage (Section 4.1), with very low potential for organic matter generation and discharge of hydrocarbons and even carbonation, which, combined with stronger diagenesis and compaction, tends to cause the organic matter pore network to shrink and close. The lower quartz content (Section 4.2) in the Niutitang Formation suggests that quartz does not provide sufficient support and protection to organic matter pores, accelerating their destruction.

5.3.3. Tectonic Preservation Conditions

In this study, an evaluation system for the tectonic preservation of shale gas in Wufeng-Longmaxi and Niutitang shales in northern Guizhou Province was constructed based on parameters such as stratigraphic dip, fracture and fold development, depth of burial, the thickness of cover and top and bottom plates, the degree of slip tectonics, the development and degree of denudation, etc. Based on this evaluation system, the influence of tectonic preservation conditions on pore structure and gas content in different reservoirs was studied. The comprehensive evaluation refers to evaluating the relative quality of the shale gas preservation conditions of the Wufeng-Longmaxi and Niutitang Formations according to the multiple evaluation indicators of shale gas preservation conditions in Table 11. Compared with a poor comprehensive evaluation, a good comprehensive evaluation means that the preservation conditions are better, and the degree of multi-phase tectonic transformation is weaker, which is more conducive to the preservation of shale gas.

Table 11. Comprehensive evaluation of the tectonic preservation conditions of the Wufeng-Longmaxi and Niutitang Formations in northern Guizhou Province.

Evaluation Parameters	Daozhen Syncline	Xieba Anticlinorium
Target Stratum	**Wufeng-Longmaxi Formation**	**Niutitang Formation**
Cover thickness	220	135
High-quality shale thickness/m	28	8
Number of natural fractures	6	25
Stratum dip/°	19.5	65
Average depth/m	2800	650
Formation breakthrough pressure/MPa	20.4	19.5
Fractures	Undeveloped	Well developed
Fold	NE, NNE	NE, NNE
Denudation degree	Weak	Intense
Comprehensive evaluation	Good	Poor

The gas-producing layer of the Daozhen syncline has a larger cover thickness (Table 11), which effectively prevents the escape of shale gas in Wufeng-Longmaxi shale and is far from hydrothermal deposits. In addition, the stratigraphic dip is small, which is beneficial for slowing the vertical migration of shale gas. The thickness of Xieba anticlinorium cover in northern Guizhou Province is smaller, the stratigraphic depth is shallower, the stratigraphic dip is larger, the stratigraphic breakout pressure is smaller, the thickness of high-quality shale is smaller, the regional fractures are more developed, and the tectonic pattern is broad and slow, but faults and high-angle fractures are generally developed, and the layer is highly stripped, leading to poor shale gas preservation conditions.

In terms of microscopic pore structure, the pore volume, mercury porosity, mean throat radius, and macropore-dominant pore size (Section 5.2) of Wufeng-Longmaxi shale are all better than those of the Niutitang shale, and the good macroscopic tectonic preservation conditions match the more favorable microscopic pore structure, resulting in the gas-bearing capacity of Wufeng-Longmaxi shale in the Daozhen syncline being better than that of the Niutitang Formation in the Xieba anticlinorium reservoirs (Figure 13).

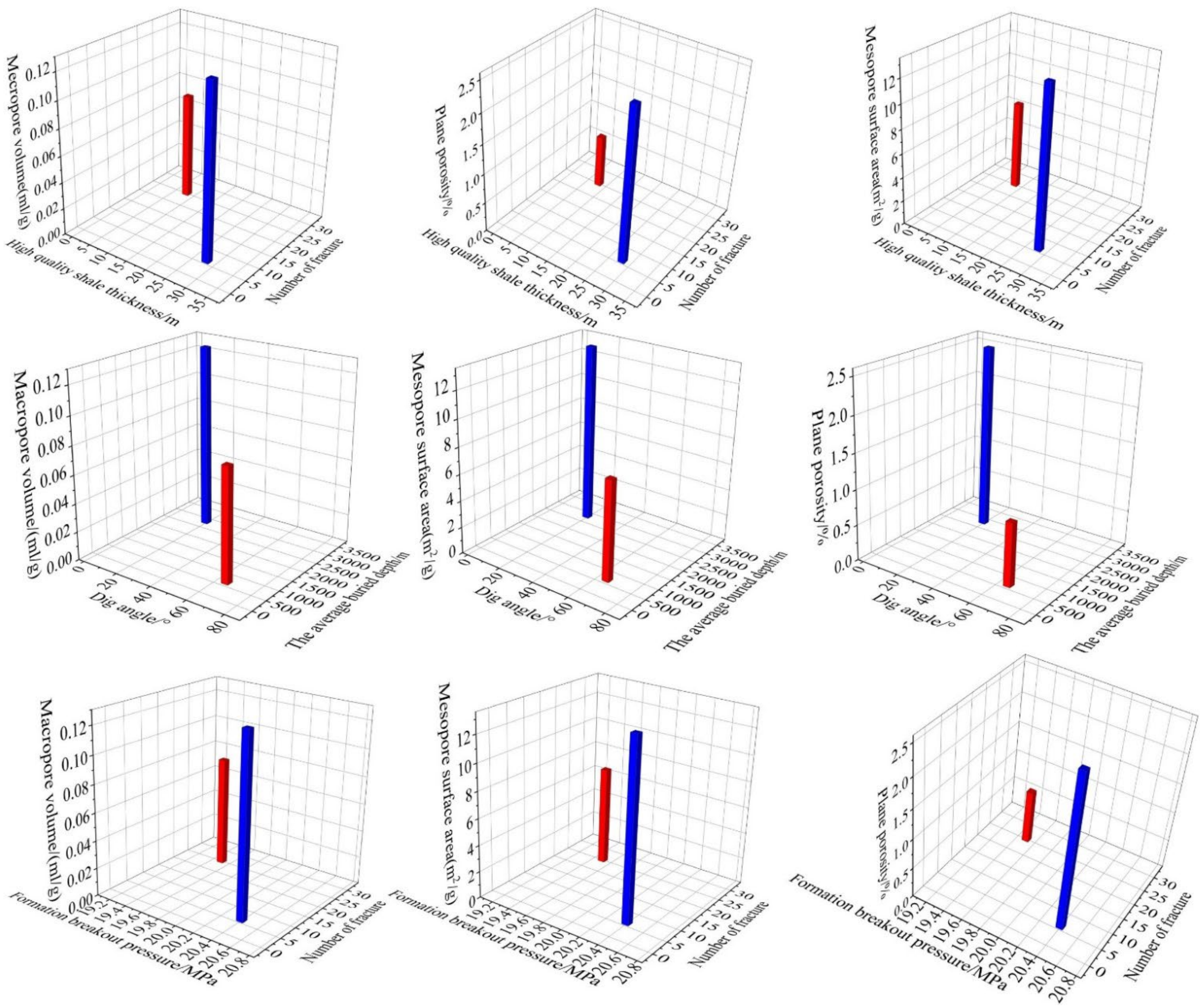

Figure 13. Relationship between tectonic preservation parameters and pore structure of the Wufeng-Longmaxi Formation and the Niutitang Formation in northern Guizhou Province (The blue bars represent the Wufeng-Longmaxi Formation, and the red bar represent the Niutitang Formation).

5.4. New Insights into a Differential Reservoir-Forming Model for Lower Paleozoic Marine Gas Shales

Through comprehensive analyses, we established a differential reservoir-forming model based on diagenesis and the depositional environment, the degree of thermal evolution, and tectonism (Figure 14).

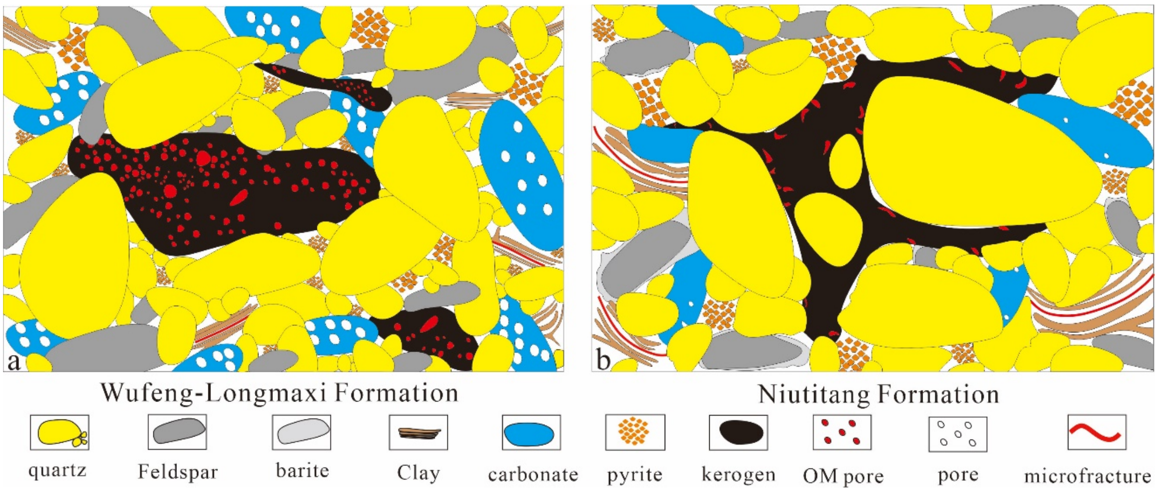

Figure 14. Proposed conceptual model for elaborating differential reservoir-forming mechanisms for the Lower Paleozoic Wufeng-Longmaxi and Niutitang Formations. (**a**) Wufeng-Longmaxi Formation; (**b**) Niutitang Formation.

The reservoir-forming model of organic matter pores presents obvious differences between Wufeng-Longmaxi and Niutitang Formation shales in northern Guizhou Province. The Wufeng-Longmaxi shale is at a high thermal maturity. The organic matter pores are all nanoscale pores with a concentrated range of pore sizes; a variety of organic pore structure parameters indicate that the organic pore morphology is relatively regular and less rough, and the support of more quartz particles has improved the development and preservation of organic pores. In addition, the interaction between organic acids and carbonate minerals during the massive hydrocarbon production process has led to the development of more dissolution pores within the carbonate grains, and clay minerals have developed smaller and flatter intergranular microfractures.

The organic matter of Niutitang shale is at the late over-mature evolutionary stage, and the pore size and range of organic matter pores are increased. A variety of organic matter pore structure parameters indicate that the organic pore form in the Niutitang Formation is more irregular, and the pore walls are rougher. Specifically, the roundness of the organic matter pores in Niutitang shale samples (7.298 and 8.747) is greater than that in the Wufeng-Longmaxi shale (5.007), and the elongation of organic matter pores in Niutitang shale samples (2.057 and 1.778) is greater than that in the Wufeng-Longmaxi shale (1.554). In addition, the convex degree of organic matter pores in Niutitang shale samples (19.030 and 46.964) is greater than that in the Wufeng-Longmaxi shale (15.941). The reduction in the hydrocarbon generation potential of the organic matter led to a decrease in organic acid, which caused the dissolution pores to be destroyed or be filled with a lower amount of carbonate minerals and the pore size to become significantly smaller. The deeper depth of the Niutitang Formation indicates more intense compaction, and lower clay mineral content has resulted in the development of more curved microfractures. The comprehensive analysis of the reservoir-forming model of organic matter pores shows that the pore structure of the Wufeng-Longmaxi Formation is better than that of the Niutitang shale, and ultimately, the microscopic pore structure is characterized by a higher gas content in well Daoye 1 in the Daozhen syncline (1.48 m^3/t) compared to that in well Zhengye 1 in the Xieba anticlinorium (1.28 m^3/t).

6. Conclusions

The organic matter of the Wufeng-Longmaxi Formation in northern Guizhou Province is in the stage of high-maturity evolution, and the whole shale belongs to siliceous litho-facies, while some samples belong to mixed clayey–siliceous shale facies, which mainly developed organic matter pores, intergranular pores of minerals, dissolution pores of carbonate minerals, intergranular fractures, and microcracks of clay minerals. The organic matter in Niutitang shale is in the over-mature evolution stage and belongs to siliceous lithofacies, which mainly developed organic matter pores and intergranular pore fractures of clay minerals. The main pore size distribution range of Wufeng-Longmaxi shale is larger than that of Niutitang shale, and ink-bottle pores are more developed with a smaller macropore specific surface area. The plane porosity of organic matter in Wufeng-Longmaxi shale is higher than that of Niutitang shale, which shows that Ro, clay mineral content, and TOC all control the plane porosity of the Wufeng-Longmaxi shale reservoir.

The differential accumulation process of shale gas in Wufeng-Longmaxi and Niutitang shales in northern Guizhou Province is mainly controlled by lithofacies, the thermal evolution degree, and tectonic preservation conditions. Higher clay mineral content in Wufeng-Longmaxi shale led to more intergranular pores with clay minerals, and more carbonate mineral content promoted the development of dissolution pores and formed more ink-bottle pores, which have greatly improved the adsorption capacity of the reservoir to shale gas. The lower plane porosity of Niutitang Formation shale reservoirs reflects the compaction and cementation of overlying strata under pressure, which destroyed the pore space and developed high-angle fractures at the same time. The organic matter of the Wufeng-Longmaxi shale is at a high-maturity stage, with well-developed organic pores. The organic matter of the Niutitang Formation is at the over-mature stage, and the hydrocarbon generation capacity of organic matter has greatly decreased, while the greater compaction has destroyed the pore space. Compared with the Xieba anticlinorium, the larger cover layer thickness, smaller stratigraphic dip, smaller fracture distribution, thicker organic shale stratum thickness, larger strata breakthrough pressure, and weaker denudation conditions provide better preservation conditions in Wufeng-Longmaxi shale; the higher gas content also supports this view.

In this study, the types and structural characteristics of shale reservoir space in the Wufeng-Longmaxi and Niutitang Formations in northern Guizhou Province were compared, and the differential accumulation mechanisms of shale gas between the two formations were revealed, which laid the foundation for determining the main controlling factors of differential shale gas enrichment. Finally, a differential reservoir-forming model for the Lower Paleozoic marine gas shales was established, which provides a theoretical basis for the commercial development of shale gas in northern Guizhou Province.

Author Contributions: Funding acquisition, F.S.; Investigation, W.D., R.L., Y.W., D.Z., Y.C., Z.S. and F.Z.; Methodology, F.S., R.L., Y.W., D.Z., Y.C., Z.S. and F.Z.; Project administration, F.S.; Supervision, W.Y. and X.L.; Writing—original draft, W.D.; Writing—review & editing, W.Y. and X.L. All authors have read and agreed to the published version of the manuscript.

Funding: This research was funded by the [Guizhou Geological Exploration Foundation] grant number [208-9912-JBN-L1D7], [the Natural Science Foundation of China] grant number [42172140], [the Science Foundation for Distinguished Young Scholars of China University of Petroleum, Beijing] grant number [2462020QNXZ004], [the Research Project funded by Guizhou Research Institute of Petroleum Exploration and Development] grant number [GZYQY-2021008] and [China National Major Project of Science and Technology] grant number [2016ZX05034-001 and 2017ZX05035-002] And The APC was funded by [Natural Science Foundation of China: 42172140; Science Foundation for Distinguished Young Scholars of China University of Petroleum, Beijing: 2462020QNXZ004; Guizhou Research Institute of Petroleum Exploration and Development: GZYQY-2021008; China National Major Project of Science and Technology: 2016ZX05034-001 and 2017ZX05035-002].

Data Availability Statement: Not applicable.

Acknowledgments: This work was mainly financed by the Natural Science Foundation of China (Grant No. 42172140), the Science Foundation for Distinguished Young Scholars of China University of Petroleum, Beijing (No. 2462020QNXZ004), the Research Project funded by Guizhou Research Institute of Petroleum Exploration and Development (Grant. GZYQY-2021008), and China National Major Project of Science and Technology (Grant. 2016ZX05034-001 and 2017ZX05035-002). Thanks to Bing Yang, Deputy Director of the Department of Natural Resources, for his guidance and support for this research.

Conflicts of Interest: The authors declare that they have no known competing financial interest or personal relationships that could have appeared to influence the work reported in this paper.

References

1. Dong, D.Z.; Zou, C.N.; Li, J.Z.; Wang, S.J.; Li, X.J.; Wang, Y.M.; Li, D.H.; Huang, J.L. Resource potential, exploration and development prospect of shale gas in the whole world. *Geol. Bull. China* **2011**, *30*, 324–336.
2. Kang, Y.Z. Significant Exploration Progress and Resource Potential of Unconventional Oil and Gas in China. *Pet. Sci. Technol. Forum* **2018**, *37*, 1–7.
3. Nie, H.K.; Tang, X.; Bian, R.K. Controlling factors for shale gas accumulation and prediction of potential development area in shale gas reservoir of South China. *Acta Pet. Sin.* **2009**, *30*, 484–491.
4. Zhang, J.C.; Xu, B.; Nie, H.K.; Wang, Z.Y.; Lin, T. Exploration potential of shale gas resources in China. *Nat. Gas Ind.* **2008**, *28*, 136–140.
5. Zhang, J.C.; Nie, H.K.; Xu, B.; Jiang, S.L.; Zhang, P.X.; Wang, Z.Y. Geological condition of shale gas accumulation in Sichuan Basin. *Nat. Gas Ind.* **2008**, *28*, 151–156.
6. Yang, X. The Study on Reservoir Characteristics and Storage Capacity Dominant Factors on Shale of Lower Palaeozoic Erathem in Southeastern Chongqing Area. Master's Thesis, China University of Petroleum, Beijing, China, 2016.
7. Zhuang, T.S.; Yang, Y.; Gong, Q.S.; Xing, L.; Wei, X.F. Characteristics and Mechanisms of the Micro-pores in the Early Palaeozoic Marine Shale, Southern Sichuan Basin. *Acta Geol. Sin.* **2014**, *88*, 1728–1740.
8. Yang, F.; Ning, Z.F.; Wang, Q.; Zhang, R.; Krooss, B.M. Pore structure characteristics of lower Silurian shales in the southern Sichuan Basin, China: Insights to pore development and gas storage mechanism. *Int. J. Coal Geol.* **2016**, *156*, 12–24. [CrossRef]
9. Yang, P.P. Pore Structure Characterization and Its Control Factors of the Lower Cambrian Niutitang Formation Shale in Northeast Chongqing. Master's Thesis, China University of Petroleum, Beijing, China, 2016.
10. He, Q.; He, S.; Dong, T.; Zhai, G.Y.; Wang, Y.; Wan, K. Pore structure characteristics and controls of Lower Cambrian Niutitang Formation, western Hubei Province. *Pet. Geol. Exp.* **2019**, *41*, 530–539.
11. Meng, P.F. Whole-aperture characteristics of the Niutitang Formation shale in the Western Hunan-Hubei area. *China Energy Environ. Prot.* **2017**, *39*, 119–125. [CrossRef]
12. Chen, S.B.; Zhu, Y.M.; Wang, H.Y.; Liu, H.L.; Wei, W.; Fang, J.H. Structure characteristics and accumulation significance of nanopores in Longmaxi shale gas reservoir in the southern Sichuan Basin. *J. China Coal Soc.* **2012**, *37*, 438–444.
13. Guo, X.S.; Li, Y.P.; Liu, R.B.; Wang, Q.B. Characteristics and controlling factors of micro-pore structures of Longmaxi Shale Play in the Jiaoshiba area, Sichuan Basin. *Nat. Gas Ind.* **2014**, *34*, 9–16.
14. Li, X.Q.; Wang, Y.; Guo, M.; Zhang, J.Z.; Zhao, P.; Xu, H.W.; Yang, J.; Wang, F.Y. Pore Characteristics of Shale Gas Reservoirs from the Lower Paleozoic in the South of Sichuan Basin. *Nat. Gas Geosci.* **2015**, *26*, 1464–1471.
15. Peng, N.; He, S.; Hao, F.; He, X.; Zhang, P.; Zhai, G.; Bao, S.; He, C.; Yang, R. The Pore Structure and Difference between Wufeng and Longmaxi Shales in Pengshui Area, Southeastern Sichuan. *Earth Sci.* **2017**, *42*, 1134–1146.
16. Loucks, R.G.; Reed, R.M.; Ruppel, S.C.; Jarvie, D.M. Morphology, Genesis, and Distribution of Nanometer-Scale Pores in Siliceous Mudstones of the Mississippian Barnett Shale. *J. Sediment. Res.* **2009**, *79*, 848–861. [CrossRef]
17. Chalmers, G.R.; Bustin, R.M.; Power, I.M. Characterization of gas shale pore systems by porosimetry, pycnometry, surface area, and field emission scanning electron microscopy/transmission electron microscopy image analyses: Examples from the Barnett, Woodford, Haynesville, Marcellus, and Doig units. *AAPG Bull.* **2012**, *96*, 1099–1119. [CrossRef]
18. Ambrose, R.J.; Hartman, R.C.; Diaz-Campos, M.; Akkutlu, I.Y.; Sondergeld, C.H. New Pore-scale Considerations for Shale Gas in Place Calculations. In Proceedings of the SPE Unconventional Gas Conference, Pittsburgh, PA, USA, 23–25 February 2010.
19. Curtis, M.E. Structural Characterization of Gas Shales on the Micro- and Nano-Scales. In Proceedings of the Canadian Unconventional Resources and International Petroleum Conference, Calgary, AB, Canada, 19–21 October 2010.
20. Curtis, M.E.; Sondergeld, C.H.; Ambrose, R.J.; Rai, C.S. Microstructural investigation of gas shales in two and three dimensions using nanometer-scale resolution imaging. *AAPG Bull.* **2012**, *96*, 665–677. [CrossRef]
21. Sondergeld, C.H.; Ambrose, R.J.; Rai, C.S.; Moncrieff, J. Micro-Structural Studies of Gas Shales. In Proceedings of the SPE Unconventional Gas Conference, Pittsburgh, PA, USA, 23–25 February 2010.
22. Zhao, D.F. Quantitative Characterization of Pore Structure of Shale Reservoirs in the Lower Paleozoic Wufeng-Longmaxi formation of the East Sichuan Area. Ph.D. Thesis, China University of Mining and Technology, Beijing, China, 2020.
23. Bernard, S.; Wirth, R.; Schreiber, A.; Schulz, H.-M.; Horsfield, B. Formation of nanoporous pyrobitumen residues during maturation of the Barnett Shale (Fort Worth Basin). *Int. J. Coal Geol.* **2012**, *103*, 3–11. [CrossRef]

24. Loucks, R.G.; Reed, R.M.; Ruppel, S.C.; Hammes, U. Spectrum of pore types and networks in mudrocks and a descriptive classification for matrix-related mudrock pores. *AAPG Bull.* **2012**, *96*, 1071–1098. [CrossRef]
25. Milliken, K.L.; Rudnicki, M.; Awwiller, D.N.; Zhang, T. Organic matter–hosted pore system, Marcellus Formation (Devonian), Pennsylvania. *AAPG Bull.* **2013**, *97*, 177–200. [CrossRef]
26. Zhao, J.; Jin, Z.; Hu, Q.; Liu, K.; Jin, Z.; Hu, Z.; Nie, H.; Du, W.; Yan, C.; Wang, R. Mineral composition and seal condition implicated in pore structure development of organic-rich Longmaxi shales, Sichuan Basin, China. *Mar. Pet. Geol.* **2018**, *98*, 507–522. [CrossRef]
27. Jarvie, D.M.; Hill, R.J.; Ruble, T.E.; Pollastro, R.M. Unconventional shale-gas systems: The Mississippian Barnett Shale of north-central Texas as one model for thermogenic shale-gas assessment. *AAPG Bull.* **2007**, *91*, 475–499. [CrossRef]
28. Liu, H.; Cao, T.T.; Qi, M.H.; Qang, D.Q.; Deng, M.; Cao, Q.G.; Cheng, B.; Liao, Z.W. Reservoir characteristics of Longtan Formation shale gas in Huayingshan area, eastern Sichuan Basin. *Nat. Gas Geosci.* **2019**, *30*, 11–26.
29. Wei, X.F.; Liu, R.B.; Zhang, T.S.; Liang, X. Micro-pores Structure Characteristics and Development Control Factors of Shale Gas Reservoir:A Case of Longmaxi Formation in XX Area of Southern Sichuan and Northern Guizhou. *Nat. Gas Geosci.* **2013**, *24*, 1048–1059.
30. Wang, X.M.; Liu, L.F.; Wang, Y.; Sheng, Y.; Zheng, S.S.; Luo, Z.H. Control of lithofacies on pore space of shale from Longmaxi Formation, southern Sichuan Basin. *Acta Pet. Sin.* **2019**, *40*, 1193.
31. Hu, D.F.; Zhang, H.R.; Ni, K.; Yu, G.C. Main controlling factors for gas preservation conditions of marine shales in southeastern margins of the Sichuan Basin. *Nat. Gas Ind.* **2014**, *34*, 17–23.
32. Liu, S.; Ye, Y.; Ran, B.; Jiang, L.; Li, Z.; Li, J.; Song, J.; Jiao, K.; Li, Z.; Li, Y. Evolution and implications of shale pore structure characteristics under different preservation conditions. *Pet. Reserv. Eval. Dev.* **2020**, *10*, 1–11. [CrossRef]
33. Zhao, S. The Structural Features and Lower Paleozoic of Black Shale Fracture Characteristics and Distribution in Qianbei Area. Master's Thesis, China University of Geosciences, Beijing, China, 2013.
34. Gao, Z.Y. Diagenesis Evolution of Carbonate Reservoirs in the Middle Permian of Fenggang 2 Block, Guizhou Province. Master's Thesis, Guizhou University, Guiyang, China, 2019.
35. Jiu, K.; Ding, W.L.; Li, Y.X.; Zhang, J.C.; Zeng, W.T. Structural Features in Northern Guizhou Area and Reservoir Fracture of Lower Cambrian Shale Gas. *Nat. Gas Geosci.* **2012**, *23*, 797–803.
36. Liu, Z.C.; Li, H.J.; Zhang, X.X.; Fang, K.; Luo, P.; Zhu, H.H. Distribution and evolution of sedimentary facies of the Lower Silurian Longmaxi Formation in southern Sichuan and northern Guizhou area. *Sediment. Geol. Tethyan Geol.* **2021**, *41*, 436–445.
37. Yang, X. Depositional Environment and Organic Matter Accumulation of the Lower Cambrian Niutitang Formation Shale in Northern Guizhou. Master's Thesis, China University of Geosciences, Beijing, China, 2020.
38. Sun, Y.S.; Guo, S.B. Qualitative and Quantitative Characterization of Shale Microscopic Pore Characteristics Based on Image Analysis Technology. *Adv. Earth Sci.* **2016**, *31*, 751–763.
39. Gong, X.P.; Tang, H.M.; Zhao, F.; Wang, J.J.; Xiong, H. Quantitative characterization of pore structure in shale reservoir of Longmaxi Formation in Sichuan Basin. *Lithol. Reserv.* **2016**, *28*, 48–57.
40. Chen, K.L.; Zhang, Y.S.; Liang, X.; Zhang, C.; Wang, G.C. Analysis of Shale Lithofacies and Sedimentary Environment on Wufeng Formation-Lower Longmaxi Formation on Dianqianbei Depression. *Acta Sedimentol. Sin.* **2018**, *36*, 743–755.
41. Wang, Y.M.; Wang, S.F.; Dong, D.Z.; Li, X.J.; Huang, J.L.; Zhang, C.C.; Guan, Q.Z. Lithofacies characterization of Longmaxi Formation of the Lower Silurian, southern Sichuan. *Earth Sci. Front.* **2016**, *23*, 119–133. [CrossRef]
42. Hu, Z.Q.; Du, W.; Peng, Y.M.; Zhao, J.H. Microscopic pore characteristics and the source-reservoir relationship of shale—A case study from the Wufeng and Longmaxi Formations in Southeast Sichuan Basin. *Oil Gas Geol.* **2015**, *36*, 1001–1008.
43. Jiang, Z.X.; Song, Y.; Tang, X.L.; Li, Z.; Wang, X.M.; Wang, G.Z.; Xue, Z.X.; Li, X.; Zhang, K.; Chang, J.Q.; et al. Controlling factors of marine shale gas differential enrichment in southern China. *Pet. Explor. Dev.* **2020**, *47*, 661–673. [CrossRef]
44. Wang, R.Y.; Ding, W.L.; Gong, D.J.; Zeng, W.T.; Wang, X.H.; Zhou, X.H.; Li, A.; Xiao, Z.K. Development characteristics and major controlling factors of shale fractures in the Lower Cambrian Niutitang Formation, southeastern Chongqing-northern Guizhou area. *Acta Pet. Sin.* **2016**, *37*, 832.
45. Xue, B.; Zhang, J.C.; Tang, X.; Yang, C.; Chen, Q.; Man, X.J.; Dang, W. Micro-pore Structure and Gas Accumulation Characteristics of Shale in the Longmaxi Formation, Northwest Guizhou. *Pet. Res.* **2016**, *1*, 191–204. [CrossRef]
46. Ma, M.; Chen, G.J.; Xu, Y.; Hu, S.J.; Lv, C.F.; Xue, L.H. Fractal characteristics of pore structure of continental shale in the process of thermal evolution. *Coal Geol. Explor.* **2017**, *45*, 41–47.
47. Ross, D.J.K.; Marc Bustin, R. The importance of shale composition and pore structure upon gas storage potential of shale gas reservoirs. *Mar. Pet. Geol.* **2009**, *26*, 916–927. [CrossRef]
48. Sing, K.S.W. Reporting physisorption data for gas/solid systems with special reference to the determination of surface area and porosity (Recommendations 1984). *Pure Appl. Chem.* **1985**, *57*, 603–619. [CrossRef]
49. Topór, T.; Derkowski, A.; Ziemiański, P.; Szczurowski, J.; McCarty, D.K. The effect of organic matter maturation and porosity evolution on methane storage potential in the Baltic Basin (Poland) shale-gas reservoir. *Int. J. Coal Geol.* **2017**, *180*, 46–56. [CrossRef]
50. Yang, X.; Jiang, Z.X.; Song, Y.; Huang, H.X.; Tang, X.L.; Ji, W.M.; Li, Z.; Wang, P.F.; Chen, L. A Comparative Study on Whole-aperture Pore Structure Characteristics between Niutitang and Longmaxi Formation of High-matruity Marine Shales in Southeastern Chongqingelt. *Geol. J. China Univ.* **2016**, *22*, 368–377. [CrossRef]

51. Wang, R.; Hu, Z.; Long, S.; Liu, G.; Zhao, J.; Dong, L.; Du, W.; Wang, P.; Yin, S. Characteristics of fractures and their significance for reservoirs in Wufeng- Longmaxi shale, Sichuan Basin and its periphery. *Oil Gas Geol.* **2021**, *42*, 1295–1306.
52. Nie, H.K.; Bian, R.K.; Zhang, P.X.; Gao, B. Micro-types and characteristics of shale reservoir of the Lower Paleozoic in Southeast Sichuan Basin, and their effects on the gas content. *Earth Sci. Front.* **2014**, *21*, 331–343. [CrossRef]